MATHEMATICS OF COMPUTATION
Volume 80, Number 274, April 2011, Pages 669–695
S 0025-5718(2010)02412-3
Article electronically published on August 26, 2010

DIVERGENCE-FREE FINITE ELEMENTS ON TETRAHEDRAL GRIDS FOR $k \geq 6$

SHANGYOU ZHANG

ABSTRACT. It was shown two decades ago that the P_k-P_{k-1} mixed element on triangular grids, approximating the velocity by the continuous P_k piecewise polynomials and the pressure by the discontinuous P_{k-1} piecewise polynomials, is stable for all $k \geq 4$, provided the grids are free of a nearly-singular vertex. The problem with the method in 3D was posted then and remains open. The problem is solved partially in this work. It is shown that the P_k-P_{k-1} element is stable and of optimal order in approximation, on a family of uniform tetrahedral grids, for all $k \geq 6$. The analysis is to be generalized to non-uniform grids, when we can deal with the complicity of 3D geometry.

For the divergence-free elements, the finite element spaces for the pressure can be avoided in computation, if a classic iterated penalty method is applied. The finite element solutions for the pressure are computed as byproducts from the iterate solutions for the velocity. Numerical tests are provided.

1. INTRODUCTION

Rewriting the Navier-Stokes or the Stokes equations in the weak variational forms, the primitive unknowns, the velocity and the pressure, belong to Sobolev spaces H^1 and L^2, respectively. Naturally, a finite element method would be the P_k-P_{k-1} element which approximates the velocity in an H^1-subspace of continuous P_k piecewise polynomials (C_0-P_k) and approximates the pressure in an L^2-subspace of discontinuous P_{k-1} piecewise polynomials (C_{-1}-P_{k-1}). This is a truly conforming element as the incompressibility condition is satisfied pointwise and the discrete solution for the velocity is a projection within the space of divergence-free functions. A fundamental study on the method was done by Scott and Vogelius ([11, 12]) that the method is stable and consequently of the optimal order on 2D triangular grids for any $k \geq 4$, provided that the grids have no nearly-singular vertex. A 2D vertex of a triangulation is singular if all edges meeting at the vertex form two cross lines; see Figure 1. For $k \leq 3$, Scott and Vogelius showed that the P_k-P_{k-1} element would not be stable, and may not produce approximating solutions on general 2D triangular grids in [11, 12]. What is this magic number k in 3D? Scott and Vogelius posted this question explicitly after discovering that $k = 4$ in 2D. The problem has remained open for more than 20 years.

The geometry of the 3D tetrahedral grids is much more complicated than that of 2D. By adding or moving a few edges and vertices locally, one can easily eliminate

Received by the editor June 18, 2008 and, in revised form, January 25, 2010.
2010 *Mathematics Subject Classification.* Primary 65N30, 76M10, 76D07.
Key words and phrases. Mixed finite elements, Stokes equations, divergence-free element, tetrahedral grids.

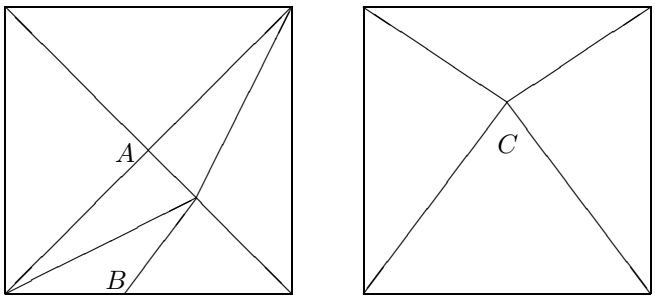

FIGURE 1. Singular vertices (A and B) and a nearly-singular vertex (C, when $C \to A$), in 2D.

singular vertices in 2D; see Figure 1. When a triangulation is singular-vertex free, it is shown by Scott and Vogelius [11, 12] that the divergence of a C_0-P_k vector space is exactly the space of C_{-1}-P_{k-1} modulus a constant. Following this approach, we found previously that this is true on Hsieh-Clough-Tocher tetrahedral grids ([17]) for all $k \geq 3$ in 3D also. For general tetrahedral grids, it is challenging to identify all the singular vertices and edges. For example, when doing multigrid refinements on tetrahedral grids (cf. [16]), a known type of singular edges (all face triangles meeting at the edge fall into two planes) and singular vertices (all face triangles meeting at the vertex fall into three planes) cannot be avoided. To extend the Scott-Vogelius result to 3D while avoiding the technical details on the geometry of singular vertices, we limit this research on a family of uniform grids, shown in Figure 2. We will show that the P_k-P_{k-1} element is stable and provides the optimal order solutions, for all $k \geq 6$. When a classic iterated penalty method ([6, 3, 4, 14]) is used here, we only need to solve a vector-Laplacian equation for the velocity with an iteration number independent of grid size. In such a case, the mixed element is reduced to a single element, and the pressure is computed as a byproduct. This research is still far away from answering the question on the magic number k in 3D proposed by Scott and Vogelius. Since we limit our work on the uniform grids, the magic k may be greater than 6. As we require $k \geq 6$ in our constructional proof, the magic k could be less than 6 as well, though unlikely; see Corollary 3.1 and the numerical result following that. We note that for the continuous pressure version of the P_k-P_{k-1} element ($k \geq 2$) on tetrahedral grids, the analysis is done in [2], extending the Taylor-Hood element [10].

The rest of the paper is organized as follows. In Section 2, we define the P_k-P_{k-1} element. In Section 3, we will prove the stability of the P_k-P_{k-1} element on a uniform grid, and show the optimal order of convergence. In Section 4, we provide some numerical results.

2. The P_k-P_{k-1} element

In this section, we shall define the P_k-P_{k-1} finite element for the stationary Stokes equations. The resulting linear systems are guaranteed to have a unique solution, i.e. the (reduced) inf-sup condition always holds for such a divergence-free finite element pair. The classic iterated penalty method ([6, 3, 4, 14]) can be applied where the mixed element is reduced to a single divergence-free element.

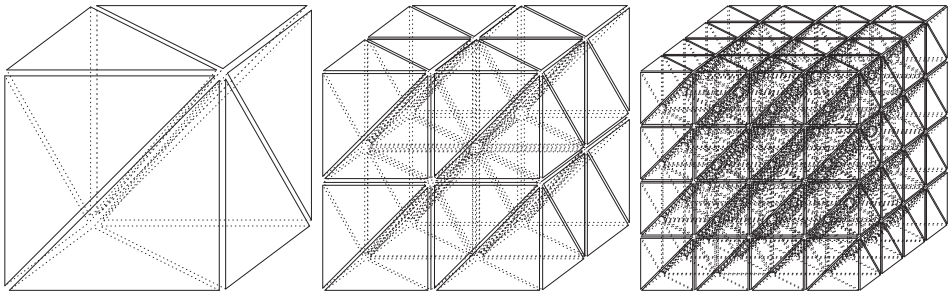

FIGURE 2. The first three levels ($n = 1, 2, 4$) of grids, Ω_h.

We solve a model stationary Stokes problem: Find functions $\mathbf{u}$ (the fluid velocity) and p (the pressure) on a domain of unit cube $\Omega = (0,1)^3$ such that

$$\begin{aligned} -\Delta \mathbf{u} + \nabla p &= \mathbf{f} && \text{in } \Omega, \\ \operatorname{div} \mathbf{u} &= 0 && \text{in } \Omega, \\ \mathbf{u} &= \mathbf{0} && \text{on } \partial\Omega, \end{aligned} \tag{2.1}$$

where $\mathbf{f}$ is the body force. The standard variational form is: Find $\mathbf{u} \in H_0^1(\Omega)^3$ and $p \in L_0^2(\Omega)$ such that

$$\begin{aligned} a(\mathbf{u}, \mathbf{v}) + b(\mathbf{v}, p) &= (\mathbf{f}, \mathbf{v}) \quad \forall \mathbf{v} \in H_0^1(\Omega)^3, \\ b(\mathbf{u}, q) &= 0 \qquad \forall q \in L_0^2(\Omega). \end{aligned} \tag{2.2}$$

Here $H_0^1(\Omega)^3$ is the Sobolev space (cf. [5]) with zero boundary trace, $L_0^2(\Omega)$ is the L^2 space with zero mean value, i.e., $L^2(\Omega)/R = \{p \in L^2 \mid \int_\Omega p = 0\}$, and

$$\begin{aligned} a(\mathbf{u}, \mathbf{v}) &= \int_\Omega \nabla \mathbf{u} \cdot \nabla \mathbf{v} \, d\mathbf{x}, \\ b(\mathbf{v}, p) &= -\int_\Omega \operatorname{div} \mathbf{u} \, p \, d\mathbf{x}, \\ (\mathbf{f}, \mathbf{v}) &= \int_\Omega \mathbf{f} \, \mathbf{v} \, d\mathbf{x}. \end{aligned}$$

Let Ω_h be a family of uniform tetrahedral grids on Ω depicted in Figure 2:

$$\Omega_h = \{K \mid K \text{ is a tetrahedron with size } \ |K| \le h\}.$$

Then we define the P_k-P_{k-1} mixed element spaces by

$$\mathbf{V}_{h,k} = \left\{\mathbf{u}_h \in C(\Omega) \mid \mathbf{u}_h|_K \in P_k(K)^3 \ \forall K \in \Omega_h \text{ and } \ \mathbf{u}_h|_{\partial\Omega} = 0\right\} \subset H_0^1(\Omega)^3, \tag{2.3}$$

$$P_h = \{\operatorname{div} \mathbf{u}_h \mid \mathbf{u}_h \in \mathbf{V}_{h,k}\} \subset L_0^2(\Omega). \tag{2.4}$$

It is widely known that the pointwise divergence-free mixed method is too complicated and not practical; cf. [4]. Very little work has been done on this method; cf. [1, 7, 8, 9, 11, 17, 18]. The resulting system of finite element equations for (2.2) is: Find $\mathbf{u}_h \in \mathbf{V}_{h,k}$ and $p_h \in P_h$ such that

$$\begin{aligned} a(\mathbf{u}_h, \mathbf{v}) + b(\mathbf{v}, p_h) &= (\mathbf{f}, \mathbf{v}) \quad \forall \mathbf{v} \in \mathbf{V}_{h,k}, \\ b(\mathbf{u}_h, q) &= 0 \qquad \forall q \in P_h. \end{aligned} \tag{2.5}$$

The linear system of equations (2.5) always has a unique solution, in the divergence-free element method; cf. [18]. We note that P_h in (2.4) is a proper subspace of traditional C_{-1}-P_{k-1} finite element space. We will characterize it in detail below. Letting $q = \operatorname{div} \mathbf{u}_h$ in (2.5), we still have the (pointwise) divergence-free property for the finite element solution

$$\int_\Omega (\operatorname{div} \mathbf{u}_h)^2 d\mathbf{x} = b(\mathbf{u}_h, q) = 0. \tag{2.6}$$

By (2.6), the unique solution $\mathbf{u}_h$ of (2.5) is divergence-free ([10, 4, 3, 18]). It is, in fact, the $a(\cdot,\cdot)$ orthogonal projection from the divergence-free space $\mathbf{Z}$ to a subspace $\mathbf{Z}_h$, defined by,

$$\mathbf{Z} := \left\{ \mathbf{v} \in H_0^1(\Omega)^3 \mid \operatorname{div} \mathbf{v} = 0 \right\}, \tag{2.7}$$

$$\mathbf{Z}_h := \left\{ \mathbf{v} \in \mathbf{V}_{h,k} \mid \operatorname{div} \mathbf{v} = 0 \right\}. \tag{2.8}$$

As P_h may be a proper subspace of discontinuous, piecewise polynomials of degree $(k-1)$ or less, it may be difficult to find a nodal basis for P_h in some cases. But on the other side, it is the special interest of the divergence-free element method that the space P_h can be omitted in computation and the discrete solutions approximating the pressure function in the Stokes equations can be obtained as byproducts, via the iterated penalty method. This does not only simplify the coding work, but also it avoids the difficulty of solving *non-positive definite* systems of linear equations, encountered in typical mixed element methods. We refer to [6, 4, 3, 14, 18] for the iterated penalty method.

3. Stability and convergence

In this section, we will prove the inf-sup condition (3.69), i.e., the stability of the divergence-free P_k-P_{k-1} mixed element. The analysis is done by construction, based on the unit cube domain Ω and the uniform grids Ω_h, except Lemma 3.1. The convergence follows the stability routinely.

Lemma 3.1. *For any $q \in P_h$ (defined in (2.4)), $k \geq 3$, there is a function $\mathbf{v}_1 \in \mathbf{V}_{h,3}$ (defined in (2.3)) such that*

$$\int_K \operatorname{div} \mathbf{v}_1 = \int_K q \quad \forall K \in \Omega_h, \quad \textit{and} \quad \|\mathbf{v}_1\|_{H^1(\Omega)^3} \leq C \|q\|_{L^2(\Omega)}. \tag{3.1}$$

Proof. For any $q \in P_h$, by the inf-sup condition for the continuous functions (cf. [10]) there is a $\mathbf{u}_q \in H_0^1(\Omega)^3$ such that

$$\operatorname{div} \mathbf{u}_q(x,y,z) = q(x,y) \quad \text{ a.e. for } (x,y,z) \in \Omega$$

and

$$\|\mathbf{u}_q\|_{H^1} \leq C \|q\|_{L^2}.$$

We modify the Lagrange interpolation operator slightly to define a "Fortin operator" (see [4]):

$$\mathbf{I}_h \ : \ C(\Omega) \cap H_0^1(\Omega)^3 \to \mathbf{V}_{h,3}, \qquad \mathbf{I}_h \ : \ \mathbf{u}_q \mapsto \mathbf{I}_h \mathbf{u}_q,$$

$$\mathbf{I}_h \mathbf{u}_q(a_i) = \mathbf{u}_q(a_i) \text{ at all nodes except the four internal face nodes,}$$

$$\int_{(\partial K)_i} \mathbf{I}_h \mathbf{u}_q d\mathbf{x} = \int_{(\partial K)_i} \mathbf{u}_q d\mathbf{x}, \quad i = 1,2,3,4,$$

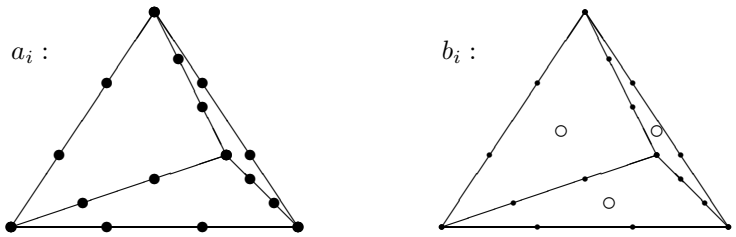

FIGURE 3. P_3 Lagrange nodes: b_i. Removing four inner-face nodes.

where $\mathbf{I}_h\mathbf{u}_q(b_i)$ (see Figure 3) is chosen so that the integral on each of the four face triangles matches that of $\mathbf{u}_q$. We note that an averaging interpolation can be adopted if the function $\mathbf{u}_q$ is not continuous, as usual; see [13]. Also follow, for example, [13], it is standard to show the stability of such an interpolation operator by scaling:

$$\|\mathbf{I}_h\mathbf{u}_q\|_{H^1} \le C\|\mathbf{u}_q\|_{H^1}.$$

The interpolant also preserves the divergence elementwise:

$$\int_K \operatorname{div}\mathbf{v}_1 d\mathbf{x} = \int_{\partial_K} \mathbf{v}_1\cdot\mathbf{n}d\mathbf{x} = \int_{\partial_K} \mathbf{u}_q\cdot\mathbf{n}d\mathbf{x} = \int_K \operatorname{div}\mathbf{u}_q d\mathbf{x} = \int_K q d\mathbf{x}.$$

We note that the above analysis in defining $\mathbf{I}_h\mathbf{u}_q \in \mathbf{V}_{h,3}$ is well known in showing the stability of P_3-P_0 element in 3D; cf. [17]. □

After matching the integral values of q elementwise by $\operatorname{div}\mathbf{v}_1$, we next match the vertex-values of $q - \operatorname{div}\mathbf{v}_1$.

Lemma 3.2. *For any $q \in P_h$ defined in (2.4) such that $\int_K q = 0 \quad \forall K \in \Omega_h$, $k \ge 3$, there is a function $\mathbf{v}_2 \in \mathbf{V}_{h,3}$ such that*

$$\operatorname{div}\mathbf{v}_2(a_i^K) = q(a_i^K) \quad \forall K \in \Omega_h, \tag{3.2}$$

$$\int_K \operatorname{div}\mathbf{v}_2 = 0 \quad \forall K \in \Omega_h, \tag{3.3}$$

$$\|\mathbf{v}_2\|_{H^1(\Omega)^3} \le C\|q\|_{L^2(\Omega)}. \tag{3.4}$$

Here a_i^K, $1 \le i \le 4$, are the four vertices of element K.

Proof. Let $q = \operatorname{div}\mathbf{w}_h$ for some $\mathbf{w}_h \in \mathbf{V}_{h,k}$, $k \ge 3$. From Figure 4, there are six types of vertices in Ω_h:

Type (a): Corner vertices shared by 2 tetrahedra, B, C, D, E, F, H in Figure 4,

Type (b): Corner vertices shared by 6 tetrahedra, A and G in Figure 4,

Type (c): Mid-edge vertices shared by 4 tetrahedra, I, P and R in Figure 4,

Type (d): Mid-edge vertices shared by 8 tetrahedra, J in Figure 4,

Type (e): Mid-face vertices shared by 12 tetrahedra, L, N and Q in Figure 4,

Type (f): Internal vertices shared by 24 tetrahedra, M in Figure 4,

For a Type (a) boundary vertex, such as B in Figure 4, the vector field $\mathbf{w}_h$ vanishes on the four boundary faces meeting at B; it follows that in each of the two tetrahedra sharing the vertex B, $\mathbf{w}_h$ vanishes along the three edges meeting at

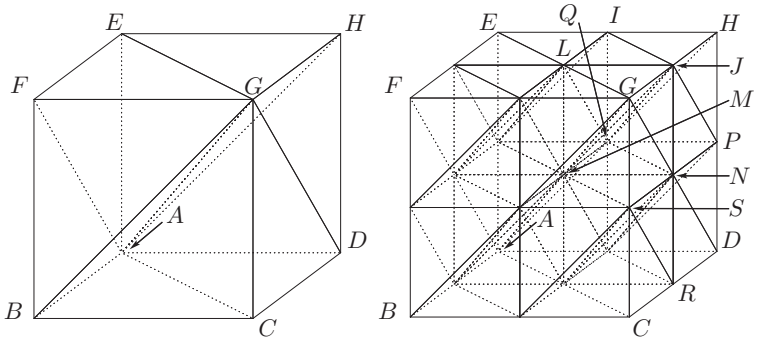

FIGURE 4. The interior and boundary vertices of Ω_h.

B (in $BASGF$, for instance, $\mathbf{w}_h$ vanishes along BA, BF, and BG). This implies that $\operatorname{div}\mathbf{w}_h = 0$ at B, so that we do not need any construction of $\mathbf{v}_2$ in order to meet the requirement (3.2), because $q|_{GAFB}(B) = q|_{GACB}(B) = 0$.

For a Type (c) vertex, similarly, all four tetrahedra meeting at the vertex have three boundary edges. Therefore, $q(a_i^{K_j}) = \operatorname{div}\mathbf{w}_h(a_i^{K_j}) = 0$ at 4 tetrahedra K_j, sharing such a boundary vertex.

For a Type (b) vertex such as A in Figure 4, there are six tetrahedra $\{K_j\}$ sharing the vertex. We define a vector function $\mathbf{v}_{2,(b)} \in P_3^3 \cap C_0(\cup K_j)$ such that $\mathbf{v}_{2,(b)} = \mathbf{0}$ at all Lagrange nodes except nodes on the diagonal edge of the cube formed by the six tetrahedra, i.e., nodes a and b in Figure 5. As $\mathbf{v}_{2,(b)}$ has three components, there are in total 6 degrees of freedom for such a $\mathbf{v}_{2,(b)}$, at nodes a and b. Note that, as $\mathbf{w}_h|_{\partial\Omega} = 0$, the gradient of $\mathbf{w}_h$ at A are the same on two tetrahedra sharing a flat boundary. That is,

$$q|_{AGEH}(A) = q|_{AGHD}(A), \quad q|_{AGDC}(A) = q|_{AGCB}(A), \quad q|_{AGBF}(A) = q|_{AGFE}(A).$$

The three values of $q(A)$ at a boundary vertex A would be matched by three degrees of freedom of $\mathbf{v}_{2,(b)}$ while the other three degrees of freedom of $\mathbf{v}_{2,(b)}$ would make $\nabla\mathbf{v}_{2,(b)} = \mathbf{0}$ at the opposite vertex G.

Let us give an explicit construction of $\mathbf{v}_{2,(b)}$. Without loss of generality, let $ABCDEFGH$ be the unit cube at the origin. Let a "derivative nodal" basis function $\phi_{(b)}(x,y,z)$ at A be the continuous piecewise P_3 function which has nodal value 0 at all Lagrange nodes except two diagonal nodes a and b (see Figure 5), so that

$$\nabla\phi_{(b)}(G) = \begin{pmatrix} 0 \\ 0 \\ 0 \end{pmatrix}, \quad \text{but} \quad \nabla\phi_{(b)}(A) = \begin{cases} \begin{pmatrix} 1 & 0 & 0 \end{pmatrix}^T & \text{on } AGEH \cup AGHD, \\ \begin{pmatrix} 0 & 0 & 1 \end{pmatrix}^T & \text{on } AGDC \cup AGCB, \\ \begin{pmatrix} 0 & 1 & 0 \end{pmatrix}^T & \text{on } AGBF \cup AGFE. \end{cases}$$

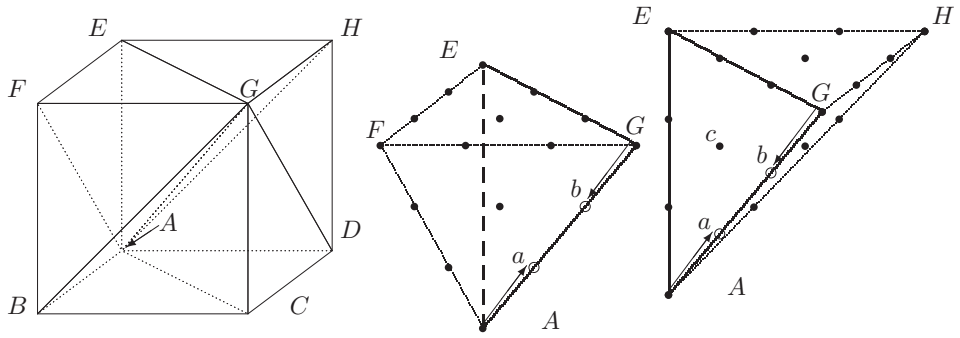

FIGURE 5. The vertices and the Lagrange interpolation nodes.

We can define (not unique) this continuous P_3 nodal basis by (see Figure 4),

$$\phi_{(b)}(x,y,z) = \begin{cases} x(1-z)(1+y-2z) & \text{on } AGEH, \\ x(1-y)(1+z-2y) & \text{on } AGHD, \\ z(1-y)(1+x-2y) & \text{on } AGDC, \\ z(1-x)(1+y-2x) & \text{on } AGCB, \\ y(1-x)(1+z-2x) & \text{on } AGBF, \\ y(1-z)(1+x-2z) & \text{on } AGFE. \end{cases} \tag{3.5}$$

The function $\mathbf{v}_{2,(b)}$ to be constructed is

$$\mathbf{v}_{2,(b)} = \phi(b)(x,y,z) \begin{pmatrix} q|_{AGEH}(A) \\ q|_{AGBF}(A) \\ q|_{AGDC}(A) \end{pmatrix}. \tag{3.6}$$

By the construction $\operatorname{div} \mathbf{v}_{2,(b)}$ has zero nodal values at all vertices of 6 K_j, except at vertex A, where the six values match that of q. By the equivalence of norms on the unit cube for piecewise polynomials, we have

$$|q(A)| \le Ch^{-3/2} \|q\|_{L^2(\bigcup K_j)}. \tag{3.7}$$

On the other side, we used scaled derivatives to define $\mathbf{v}_{2,(b)}$ and we get the following bound:

$$\begin{aligned} |\mathbf{v}_{2,(b)}|_{H^1(\bigcup K_j)^3} &\le C |\operatorname{div} \mathbf{v}_{2,(b)}|_{L^2(\bigcup K_j)} \le Ch^{3/2} |\operatorname{div} \hat{\mathbf{v}}_{2,(b)}|_{L^2((0,1)^3)} \\ &\le Ch^{3/2} |q(A)| \le C \|q\|_{L^2(\bigcup K_j)}. \end{aligned} \tag{3.8}$$

We note that due to the uniform grid, we can compute the constants in (3.7) and (3.8). For example, by (3.5) and (3.6), we can obtain

$$\begin{aligned} |\mathbf{v}_{2,(b)}|_{H^1(AGEH)^3} &= \big|q|_{AGEH}(0,0,0)\big| \sqrt{3} |x(1-z)(1+y-2z)|_{H^1(AGEH)} \\ &= \big|q|_{AGEH}(0,0,0)\big| \frac{1}{\sqrt{35}} = 2\sqrt{3} \|\operatorname{div} \mathbf{v}_{2,(b)}\|_{L^2(AGEH)}. \end{aligned}$$

But the constants in (3.7) and (3.8) would depend on the polynomial degree k.

The constructed $\mathbf{v}_{2,(b)}$ satisfies (3.2) and (3.4), but not (3.3), i.e., $\int_{K_j} \operatorname{div} \mathbf{v}_{2,(b)} \neq 0$. By the divergence theorem, the integral on the whole cube formed by the 6 tetrahedra is zero. After correcting the integrals on 5 of the 6 tetrahedron by

functions supported inside two tetrahedra each time, the last integral on the sixth integral would be zero also. First, we define $\mathbf{v}_{2,(b1)}$ by

$$\mathbf{v}_{2,(b1)} = \begin{cases} c_0 \mathbf{n}_{AGE} \phi_{AGEH} & \text{on tetrahedron } AGEH, \\ d_0 \mathbf{n}_{AGE} \phi_{AGEF} & \text{on tetrahedron } AGEF, \end{cases} \tag{3.9}$$

where $\mathbf{n}_{AGE}$ is the outward normal to the face AGE on tetrahedron $AGEH$ and ϕ_{AGEH} is a P_3 polynomial identically zero on the three faces of $AGEH$ except face triangle AGE. ϕ_{AGEH} is zero on all Lagrange nodes except c; cf. Figure 5. For example, if $AGEH$ is the unit cube as in (3.6), $\phi_{AGEH} = x(1-z)(z-y)$. In (3.9), c_0 is chosen so that

$$\int_{AGEH} \operatorname{div} \mathbf{v}_{2,(b1)} d\mathbf{x} = \int_{AGEH} \operatorname{div} \mathbf{v}_{2,(b)} d\mathbf{x}. \tag{3.10}$$

In (3.9) d_0 is chosen so that $\mathbf{v}_{2,(b1)}$ is continuous on the interface. We note that c_0 can always be found to satisfy (3.10) as $\mathbf{n}_{AGE} \cdot \nabla \phi_{AGEH}$ is strictly positive inside $AGEH$ for the third degree polynomial ϕ_{AGEH}. By a scaling argument, we have also that

$$\|\mathbf{v}_{2,(b1)}\|_{H^1(\Omega)^3} \leq C \|\mathbf{v}_{2,(b)}\|_{H^1(\Omega)^3} \leq C \|q\|_{L^2(\Omega)}. \tag{3.11}$$

Next, we repeat the process on the two tetrahedra $AGFE$ and $AGFB$ to define $\mathbf{v}_{2,(b2)}$ so that

$$\int_{AGEH} \operatorname{div} \mathbf{v}_{2,(b2)} d\mathbf{x} = \int_{AGEH} \left(\operatorname{div} \mathbf{v}_{2,(b)} - \operatorname{div} \mathbf{v}_{2,(b1)} \right) d\mathbf{x}.$$

It follows by the construction that

$$\|\mathbf{v}_{2,(b2)}\|_{H^1(\Omega)^3} \leq C \|\mathbf{v}_{2,(b1)}\|_{H^1(\Omega)^3} + C \|\mathbf{v}_{2,(b)}\|_{H^1(\Omega)^3} \leq C \|q\|_{L^2(\Omega)}. \tag{3.12}$$

Repeatedly, we obtain $\mathbf{v}_{2,(bi)}$, $i = 1, 2, ..., 5$. We note that after we define $\mathbf{v}_{2,(b5)}$, the integral of the divergence of the difference $\mathbf{v}_{2,(b)} - \sum \mathbf{v}_{2,(bi)}$ has to be zero on the sixth tetrahedron as it is zero on the seventh tetrahedron which is also the first tetrahedron. Let $\tilde{\mathbf{v}}_{2,(b)} = \mathbf{v}_{2,(b)} - \sum \mathbf{v}_{2,(bi)}$. Then $\tilde{\mathbf{v}}_{2,(b)}$ satisfies (3.3) and (3.4), and its divergence matches q at 6 vertices of 6 tetrahedra at A while being zero at all other vertices. By symmetry, we can construct such a $\tilde{\mathbf{v}}_{2,(b)}$ at the other vertex G.

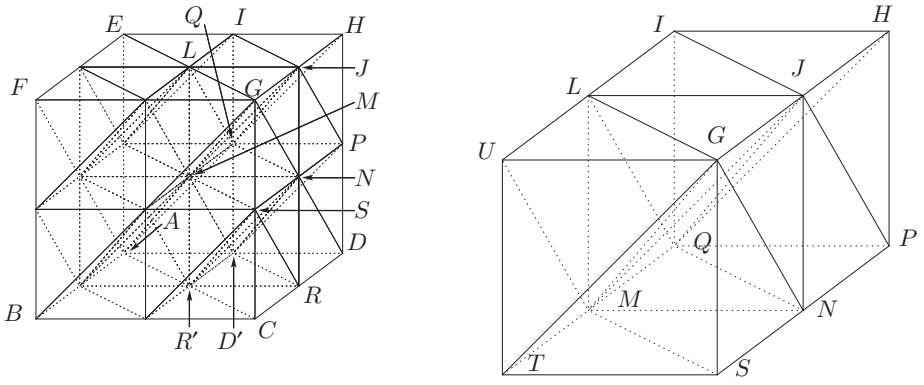

FIGURE 6. 8 tetrahedra meeting at a vertex J.

For a Type (d) vertex, for example, J in Figure 4, we construct a $\tilde{\mathbf{v}}_{2,(d)}$. This time, we have two internal edges meeting at J, on which we have 6 degrees of freedom to match $\operatorname{div}\mathbf{v}_{2,(d)}$ with q at the 8 vertices of 8 tetrahedra meeting at J. Similar to (3.5) and (3.7), we define one part of $\mathbf{v}_{2,(d)}$ as follows (cf. Figure 4).

$$\operatorname{div}\mathbf{v}_{2,(d1)}|_{ILJ}(J) = q|_{ILJ}(J) = q|_{IHJ}(J), \tag{3.13}$$

$$\operatorname{div}\mathbf{v}_{2,(d1)}|_{HPJ}(J) = q|_{NPJ}(J) = q|_{IHJ}(J), \tag{3.14}$$

$$\operatorname{div}\mathbf{v}_{2,(d1)}|_{MQLJ}(J) = q|_{MJLQ}(J) \neq q|_{MJQN}(J). \tag{3.15}$$

To do so, we repeat the construction of $\mathbf{v}_{2,(b)}$. Next, on an internal edge JM, we define a nodal basis function $\phi_{(d)}$ like (3.5):

$$\phi_{(d)} = \begin{cases} (1-y)(z-x)(-y) & \text{on } MJNG, \\ (y-x)(1-z)(-y) & \text{on } MJGL, \\ (1+x-z)(y)(-y) & \text{on } MJLQ, \\ (1+x-y)(z)(-y) & \text{on } MJQN, \end{cases}$$

assuming that M is the origin and MN is an edge in the y direction of length 1.

We construct the second part of $\mathbf{v}_{2,(d)}$ by

$$\mathbf{v}_{2,(d2)} = \phi_{(d)} \begin{pmatrix} q|_{MJNG}(J) - (q|_{MJLQ}(J) - q|_{MJQN}(J)) \\ q|_{MJNG}(J) \\ q|_{MJNG}(J) - (q|_{MJLQ}(J) - q|_{MJQN}(J)) \end{pmatrix}.$$

Then we let $\mathbf{v}_{2,(d)} = \mathbf{v}_{2,(d1)} + \mathbf{v}_{2,(d2)}$. $\operatorname{div}\mathbf{v}_{2,(d)}$ matches q at 7 vertices at J, except

$$\operatorname{div}(\mathbf{v}_{2,(d1)} + \mathbf{v}_{2,(d2)})|_{MJGL}(J) = q|_{MJNG}(J) - q|_{MJLQ}(J) + q|_{MJQN}(J).$$

Will $\operatorname{div}\mathbf{v}_{2,(d)}|_{MJGL}(J) = q|_{MJGL}(J)$? The answer is yes. As continuous P_3 functions, the gradients of three components $\mathbf{w}_h$ at J are

$$\operatorname{grad} w_{h,i} = \begin{cases} \begin{pmatrix} 0 & w_{i,1} & 0 \end{pmatrix}^T & \text{on } MJNG, \\ \begin{pmatrix} 0 & 0 & w_{i,1} \end{pmatrix}^T & \text{on } MJGL, \\ \begin{pmatrix} w_{i,2} & 0 & w_{i,1} \end{pmatrix}^T & \text{on } MJLQ, \\ \begin{pmatrix} w_{i,2} & w_{i,1} & 0 \end{pmatrix}^T & \text{on } MJQN, \end{cases}$$

where $w_{i,j}$ are constants. Then

$$\operatorname{div}\mathbf{w}_h(J) = \begin{cases} w_{2,1} & \text{on } MJNG, \\ w_{3,1} & \text{on } MJGL, \\ w_{1,2} + w_{3,1} & \text{on } MJLQ, \\ w_{1,2} + w_{2,1} & \text{on } MJQN, \end{cases}$$

i.e.,

$$\operatorname{div}\mathbf{w}_h|_{MJGL}(J) + \operatorname{div}\mathbf{w}_h|_{MJQN}(J) = \operatorname{div}\mathbf{w}_h|_{MJNG}(J) + \operatorname{div}\mathbf{w}_h|_{MJLQ}(J).$$

Hence, as $\operatorname{div}\mathbf{v}_{2,(d)}$ matches the 7 values of $q = \operatorname{div}\mathbf{w}_h$ at J, it matches the eighth value $\operatorname{div}\mathbf{w}_h|_{MJGL}(J)$. Finally, we correct the perturbation of $\mathbf{v}_{2,(d)}$ on the 8 tetrahedra by 7 bubble functions $\mathbf{v}_{2,(dj)}$ to obtain a $\tilde{\mathbf{v}}_{2,(d)}$ to preserve condition (3.3), as we did for $\tilde{\mathbf{v}}_{2,(b)}$ by $\{\mathbf{v}_{2,(bi)}\}_{1\le i\le 5}$.

For a Type (e) vertex, say, the mid-face vertex N in Figure 4. The additional directional derivative of $\mathbf{w}_h$ at N of internal edge NM will give us a P_3 nodal basis (cf. Figure 6)

$$\phi_{(e)} = \begin{cases} (1-y)(y-x)(y) & \text{on } MNGS, \\ (1-y)(y-z)(y) & \text{on } MNJG, \\ (1+x-y)(y-z)(y) & \text{on } MNQJ, \\ (1+x-y)(y)(y) & \text{on } MND'Q, \\ (1+z-y)(y)(y) & \text{on } MNR'D', \\ (1+z-y)(y-x)(y) & \text{on } MNSR', \end{cases}$$

assuming M is the origin and MN is a unit edge in the y direction. Let $\mathbf{v}_{2,(e1)}$ be

$$\phi_{(e)}\big(-q|_{MNGS}(N)\big)\begin{pmatrix}0\\1\\0\end{pmatrix}.$$

Then, as $\mathbf{w}_h$ vanishes on boundary triangles GNJ and GNS, we have that $\operatorname{div}\mathbf{w}_h|_{MNGS}(N) = \operatorname{div}\mathbf{w}_h|_{MNJG}(N)$, and that $\operatorname{div}\mathbf{v}_{2,(e1)}$ matches q at N on the two tetrahedra. Next, viewing the bottom two cubes (having face squares $CSNR$ and $NRDP$, respectively) below N together, N is a type J node. So, by the construction of $\mathbf{v}_{2,(d)}$, we match nodal values of $(q-\operatorname{div}\mathbf{v}_{2,(e1)})$ at N by a 5-dimensional space to get a $\mathbf{v}_{2,(e2)}$. Again, viewing the two cubes (having face squares $RDPN$ and $PNJH$, respectively) behind N together, this also makes N a type J node (a vertical mid-edge Type (d) node). We can define another $\mathbf{v}_{2,(e3)}$ to match its divergence with $(q - \operatorname{div}\mathbf{v}_{2,(e1)} - \operatorname{div}\mathbf{v}_{2,(e2)})$ at N. Therefore, the divergence of

$$\mathbf{v}_{3,(3)} = \mathbf{v}_{2,(e1)} + \mathbf{v}_{2,(e2)} + \mathbf{v}_{2,(e3)}$$

matches q at N, on all 12 tetrahedra. Unlike earlier cases, we do have (enough count) 12 degrees of freedom at N in $\{\mathbf{v}_h\}$ (3 components and 4 internal edges), but $\{(\operatorname{div}\mathbf{v}_h)(N)\}$ is only of dimension 8. On the other side, the twelve values of q at N would also form an eight-dimensional vector space, because $q = \operatorname{div}\mathbf{w}_h$ and we have the following four constraints:

$$q|_{MNGS}(N) = q|_{MNGL}(N), \tag{3.16}$$

$$q|_{D'NDR}(N) = q|_{D'NDP}(N), \tag{3.17}$$

$$q|_{R'NMS}(N) - q|_{R'NSR}(N) = -q|_{R'NRQ}(N) + q|_{R'ND'M}(N), \tag{3.18}$$

$$-q|_{QNJM}(N) + q|_{QNMD'}(N) = q|_{QND'P}(N) - q|_{QNPJ}(N). \tag{3.19}$$

Repeating the process (3.5)–(3.12), after correcting the integral of divergence of $\operatorname{div}\mathbf{v}_{2,(e)}$ on 12 tetrahedra by 11 bubble functions, we would obtain a $\tilde{\mathbf{v}}_{2,(e)}$ for the lemma.

For a Type (f) node, at an internal vertex M in Figure 4, we have 14 internal edges and 24 tetrahedra connected to the vertex. These $3 \times 14 = 42$ degrees of freedoms for $\mathbf{v}_{2,(f)}$ will make the divergence of it match q values at M on 24 tetrahedra. Here $\{q|_{K_i}(N)\}$ is a dimension 18 vector space, not of 24 dimensions. There are 6 constraints similar to (3.18) and (3.19), around the 6 square-diagonal edges meeting at N; cf. Figure 6. To construct $\mathbf{v}_{2,(f)}$, we first view M as two overlapping Type (e) vertices with 4 squares on the left and 4 on the right to M. Then we separate the eight squares meeting M into two groups, 4 on top and 4 at

the bottom, in order to use the construction for a type (e) boundary vertex. Of course, we can construct $\mathbf{v}_{2,(f)}$ directly by giving its explicit definition as we did for $\mathbf{v}_{2,(d)}$ and $\mathbf{v}_{2,(e)}$. Repeatedly, we correct $\mathbf{v}_{2,(e)}$ to get $\tilde{\mathbf{v}}_{2,(f)}$ to preserve (3.3). The lemma is proved by letting

$$\mathbf{v}_2 = \sum_{2 \text{ Type (b) vertices}} \tilde{\mathbf{v}}_{2,(b)} + \sum_{4(n-1) \text{ Type (d) vertices}} \tilde{\mathbf{v}}_{2,(d)} + \sum_{6(n-1)^2 \text{ Type (e) vertices}} \tilde{\mathbf{v}}_{2,(e)} + \sum_{(n-1)^3 \text{ Type (f) vertices}} \tilde{\mathbf{v}}_{2,(f)},$$

where n is the number of cubes in one direction. □

After we match the element integrals and the vertex values of $q \in P_h$, we will next match q pointwise on each edge within each element.

Lemma 3.3. *For any $q \in P_h$ defined in (2.4) such that $\int_K q = 0 \quad \forall K \in \Omega_h$, $k \geq 6$ and q vanishes at all vertices of grid Ω_h, there is a function $\mathbf{v}_3 \in \mathbf{V}_{h,k}$ such that*

$$\operatorname{div} \mathbf{v}_3|_{E_i^K} = q|_{E_i^K} \quad \forall K \in \Omega_h, \tag{3.20}$$

$$\int_K \operatorname{div} \mathbf{v}_3 = 0 \quad \forall K \in \Omega_h, \tag{3.21}$$

$$\|\mathbf{v}_3\|_{H^1(\Omega)^3} \leq C\|q\|_{L^2(\Omega)}. \tag{3.22}$$

Here E_i^K, $1 \leq i \leq 6$, are the six edges of tetrahedron K.

Proof. Let $\mathbf{w}_h \in \mathbf{V}_{h,k}$ such that $\operatorname{div} \mathbf{w}_h = q$ for a q satisfying the lemma conditions. We will construct a $\mathbf{v}_3$ matching its divergence with $\operatorname{div} \mathbf{w}_h$ at all edges. We start with an edge EA of triangle EAG; see Figure 8. As in Lemma 3.2, we first construct a $\mathbf{v}_{3,1}$ in $\mathbf{V}_{h,k}$ for $\mathbf{w}_h \in \mathbf{V}_{h,k}$, for all $k \geq 4$, matching q at edge EA. Then, we correct the integral of $\operatorname{div} \mathbf{v}_{3,1}$ by a $\mathbf{v}_{3,0}$ supported on two tetrahedra $FAGE$ and $EAGH$ in Figure 8. Regardless of the polynomial degree k in the lemma, the polynomial degree for $\mathbf{v}_{3,0}$ can be chosen exactly 6 for all $k \geq 4$. The reason is that in order to correct the elementwise divergence-free condition (3.21) while not perturbing the divergence on the edges shared by two neighboring tetrahedra, as we did in (3.10)–(3.12), we need degree 6 "bubble" polynomials which have an internal-face degree of freedom, shown in Figure 9.

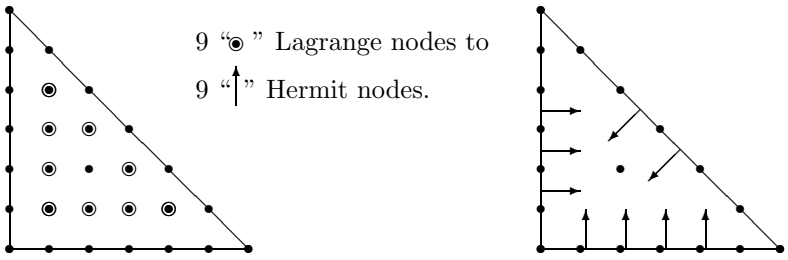

FIGURE 7. Change $\{\lambda_i = 1, \lambda_j > 0\}$ Lagrange nodes to Hermit nodes, for P_6 elements.

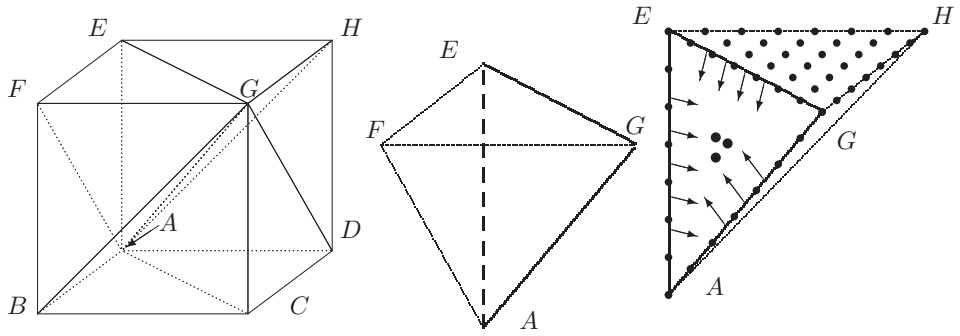

FIGURE 8. Modified Lagrange interpolation nodes for P_7.

To match the divergence of $\mathbf{w}_h$ at edge AE (see Figures 8 and 9) we replace some of the standard Lagrange interpolation nodes on the face triangle AEG by some edge-normal derivatives on the face triangle. Here we replace one loop of Lagrange nodes of the standard P_k element on one face triangle by Hermit nodes on the three edges of the triangle, shown in Figure 7 and Figure 8. We show next that the P_k element is well defined this way, for $k \geq 4$. Let $v \in P_k$ defined on tetrahedron $AEGH$ so that all interpolation values are zero. Let the restriction of v on triangle AEG be v_k. Let $L_{AE} = 0$, $L_{EG} = 0$ and $L_{GA} = 0$ be the equations for three lines AE, EG and GA, respectively. Since v_k has $(k+1)$ zero points on the three lines, we have

$$v_k = L_{AE} L_{EG} L_{GA} v_{k-3}, \quad \text{for some } v_{k-3} \in P_{k-3}(AEG)^2. \tag{3.23}$$

Let $\mathbf{n}_{L_{AE}}$ be the unit normal vector to AE inside plane EAG. As $\partial v_k / \partial \mathbf{n}_{L_{AE}}$ has $(k-2)$ zero points on the line AE (see Figures 8 and 9) $v_{k-3}|_{AE} \equiv 0$.

$$v_k = L_{AE}^2 L_{EG} L_{GA} v_{k-4}, \quad \text{for some } v_{k-4} \in P_{k-4}(AEG)^2.$$

Again, as $\partial v_k / \partial \mathbf{n}_{L_{EG}}$ has $(k-3)$ zero points on the line EG, and $\partial v_k / \partial \mathbf{n}_{L_{GA}}$ has $(k-4)$ zero points on the line GA, it follows that

$$v_k = L_{AE}^2 L_{EG}^2 L_{GA}^2 v_{k-6}, \quad \text{for some } v_{k-6} \in P_{k-6}(AEG)^2.$$

Finally, as $v = 0$ at $(k-4)(k-5)/2$ Lagrange nodes interior to triangle AEG, we conclude that $v_{k-6} \equiv 0$ and $v|_{AEG} \equiv 0$. Therefore,

$$v = L_{AEG} w_{k-1}, \quad \text{for some } w_{k-1} \in P_{k-1}(AEGH)^3. \tag{3.24}$$

Here $L_{AEG} = 0$ is an equation for the plane AEG. As the rest of the Lagrange interpolation points are not altered, $w_{k-1} = 0$ at $(k+2)(k+1)k/6$ standard Lagrange nodes for P_{k-1} in 3D (see Figure 8) we conclude that $w_{k-1} = 0$ and $v = 0$.

Now we are ready to prove the lemma. For each internal triangle, exactly one face triangle of each of two tetrahedra sharing this internal triangle are on the same plane, due to special structure of the uniform grid. For example, the edge EG of internal triangle EGA is on the plane $EFGH$ of two face triangles EFG and EGH of the two tetrahedra $EFGA$ and $EGHA$; cf. Figure 4. For internal triangle QNP, the two sharing tetrahedra have edge QN on their two face triangles plane, $IQRNJ$. If such an edge is on the boundary, then we lose all internal edge degrees of freedom

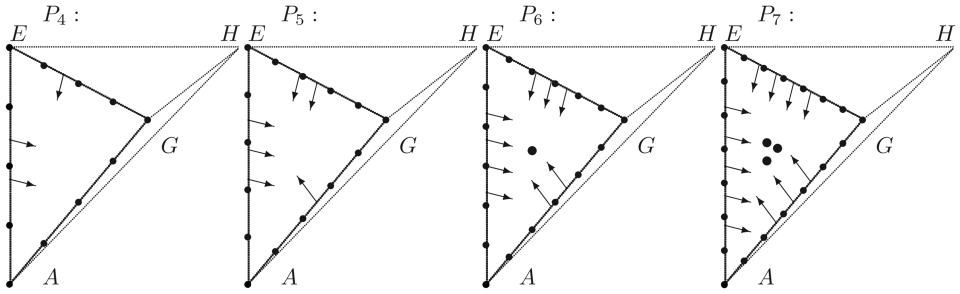

FIGURE 9. Modified Lagrange interpolation nodes for P_4, P_5, P_6 and P_7.

for $\operatorname{div} \mathbf{w}_h$ on one side of the edge, for example, $\operatorname{div} \mathbf{w}_h|_{AFE}(\mathbf{x}) = \operatorname{div} \mathbf{w}_h|_{AFB}(\mathbf{x})$ for x on edge AF; see Figure 4.

Let us first try to construct a P_4 polynomial $\mathbf{v}_3$ at two tetrahedra $GFEA$ and $GHEA$ sharing an internal triangle AEG (cf. Figure 8) to match $\operatorname{div} \mathbf{v}_3$ and $\operatorname{div} \mathbf{w}_h$ on the three edges of triangle AEG. Let us try to define a P_4 "derivative nodal basis" shown in Figure 9, which is 0 on the 6 outside face triangles of $GFEA$ and $GHEA$ and has a normal derivative 1 inside the face EAG and two normal derivatives 0 on another edge. For example, on $EAGH$, we have

$$\phi_{3,1}(x,y,z) = x(1-z)(z-y)(c_1 + c_2 x + c_3 y + c_4 z)$$

with 4 constants. But one of them is determined by the internal P_4 Lagrange node, inside the tetrahedron. The other three constants would be determined by three normal derivatives, 2 on one edge, 1 on another, 0 on the third edge, shown in Figure 9. We have three choices, EA, EG or AG, for the two-derivative edge, where the 2 normal derivatives inside triangle EAG are 0. This gives us three such "nodal basis" functions:

$$\begin{aligned}
\phi_{3,1} &= \begin{cases} \frac{27}{4} x(1-z)(z-y)x & \text{on } EAGH, \\ \frac{27}{4} y(1-z)(z-x)x & \text{on } EAGF, \end{cases} \\
\phi_{3,2} &= \begin{cases} \frac{27}{\sqrt{2}} x(1-z)(z-y)(1-z) & \text{on } EAGH, \\ \frac{27}{\sqrt{2}} y(1-z)(z-x)(1-z) & \text{on } EAGF, \end{cases} \\
\phi_{3,3} &= \begin{cases} \frac{27}{2\sqrt{2}} x(1-z)(z-y)(z-x) & \text{on } EAGH, \\ \frac{27}{\sqrt{2}} y(1-z)(z-x)(z-x) & \text{on } EAGF. \end{cases}
\end{aligned} \tag{3.25}$$

Since a $\mathbf{v}_h$ function has three components, with 3 $\phi_{3,i}$ we can have a $3 \times 3 = 9$ dimensional subspace

$$\{\mathbf{v}_h\} = \operatorname{span}\left\{ \phi_{3,i}\mathbf{e}_j \mid \mathbf{e}_1 = \begin{pmatrix} 1 \\ 0 \\ 0 \end{pmatrix},\ \mathbf{e}_2 = \begin{pmatrix} 0 \\ 1 \\ 0 \end{pmatrix},\ \mathbf{e}_3 = \begin{pmatrix} 0 \\ 0 \\ 1 \end{pmatrix} \right\}; \tag{3.26}$$

see (3.27) below. However, we need a dimension 10 $\{\operatorname{div} \mathbf{v}_h\}$ for the 10 degrees of internal-edge freedom of q on the two sides of triangle EAG. In fact, we need a dimension 12 $\{\operatorname{div} \mathbf{v}_h\}$ subspace for a general grid. But we have a special grid here that every triangle has precisely one singular edge, where the two neighboring tetrahedra have one common face plane. In this case, the edge EG is a singular

edge as $EGFA$ and $HEGA$ each have a triangle on plane $z=1$. When a singular edge is on the boundary, q is continuous on it. In particular, when $k=4$, we have $q|_{EAGF}(\frac{1}{3},\frac{1}{3},1) = q|_{EAGH}(\frac{1}{3},\frac{1}{3},1)$, and $q|_{EAGF}(\frac{2}{3},\frac{2}{3},1) = q|_{EAGH}(\frac{2}{3},\frac{2}{3},1)$; cf. Figure 8 and (3.27). To match q at these two points, we let

$$\begin{aligned}
\mathbf{v}_{3,1} &= \frac{2}{3} q|_{EAGF}(\frac{1}{3},\frac{1}{3},1) \begin{pmatrix} 0 \\ \phi_{3,1} \\ \phi_{3,1} - \sqrt{2}\phi_{3,3} \end{pmatrix}, \\
\mathbf{v}_{3,2} &= \frac{1}{3} q|_{EAGF}(\frac{2}{3},\frac{2}{3},1) \begin{pmatrix} 0 \\ -4\phi_{3,1} \\ \sqrt{2}\phi_{3,3} - 4\phi_{3,1} \end{pmatrix}.
\end{aligned} \tag{3.27}$$

In order to match the other 8 q values on the other two edges, we need to "borrow" one degree of freedom of $\mathbf{v}_h$ from the next interface. Similar to (3.27), we construct one more basis function on the next two tetrahedra:

$$\phi_{3,4} = \begin{cases} \frac{27}{4} x(1-z)(y-x)(1-y) & \text{on } AGHE, \\ \frac{27}{4} x(1-y)(z-x)(1-y) & \text{on } AGHD. \end{cases} \tag{3.28}$$

We only use one additional freedom, in addition to the 9-dimensional space (3.26)

$$\begin{pmatrix} 0 \\ \phi_{3,4} \\ 0 \end{pmatrix}$$

whose divergence is zero on all edges except on the $EAGF$ side of of edge AG. We construct $\mathbf{v}_{3,i}$ so that $\operatorname{div} \mathbf{v}_{3,i}$ match the rest of the eight degrees of freedom of q at the other two edges: edge AG:

$$\begin{aligned}
\mathbf{v}_{3,3} &= \frac{2}{3} q|_{EAGF}(\frac{1}{3},\frac{1}{3},\frac{1}{3}) \begin{pmatrix} 0 \\ \phi_{3,1} - \phi_{3,4} \\ (1/\sqrt{2})\phi_{3,2} \end{pmatrix}, \\
\mathbf{v}_{3,4} &= \frac{2}{3} q|_{EAGH}(\frac{1}{3},\frac{1}{3},\frac{1}{3}) \begin{pmatrix} \phi_{3,1} \\ \phi_{3,4} \\ 0 \end{pmatrix}, \\
\mathbf{v}_{3,5} &= -\frac{1}{3} q|_{EAGF}(\frac{2}{3},\frac{2}{3},\frac{2}{3}) \begin{pmatrix} 0 \\ 4\phi_{3,1} - \phi_{3,4} \\ (1/\sqrt{2})\phi_{3,2} \end{pmatrix}, \\
\mathbf{v}_{3,6} &= -\frac{1}{3} q|_{EAGH}(\frac{2}{3},\frac{2}{3},\frac{2}{3}) \begin{pmatrix} 4\phi_{3,1} \\ \phi_{3,4} \\ 0 \end{pmatrix},
\end{aligned} \tag{3.29}$$

and edge AE:

$$
\begin{aligned}
\mathbf{v}_{3,7} &= \frac{\sqrt{2}}{3} q|_{EAGF}(0,0,\frac{1}{3}) \begin{pmatrix} \phi_{3,2}-\phi_{3,3} \\ \sqrt{2}\phi_{3,4} \\ 0 \end{pmatrix}, \\
\mathbf{v}_{3,8} &= \frac{\sqrt{2}}{3} q|_{EAGH}(0,0,\frac{1}{3}) \begin{pmatrix} 0 \\ \phi_{3,2}-\phi_{3,3}-\sqrt{2}\phi_{3,4} \\ \phi_{3,2} \end{pmatrix}, \\
\mathbf{v}_{3,9} &= -\frac{1}{3\sqrt{2}} q|_{EAGF}(0,0,\frac{2}{2}) \begin{pmatrix} \phi_{3,2}-4\phi_{3,3} \\ \sqrt{2}\phi_{3,4} \\ 0 \end{pmatrix}, \\
\mathbf{v}_{3,10} &= -\frac{3\sqrt{2}}{q}|_{EAGH}(0,0,\frac{2}{3}) \begin{pmatrix} 0 \\ \phi_{3,2}-4\phi_{3,3}-\sqrt{2}\phi_{3,4} \\ \phi_{3,2} \end{pmatrix}.
\end{aligned} \tag{3.30}
$$

Hence, letting $\mathbf{v}_3 = \sum_{i=1}^{10} \mathbf{v}_{3,i}$, we have $\operatorname{div} \mathbf{v}_3$ zero at all vertices, and on all other edges except the three edges on two sides of triangle AEG where the divergence matches q, assuming EG is a boundary edge. We remark that we have to "borrow" a degree of freedom from next internal triangle, no matter how high the polynomial degree k is. For example, when $k = 5$, we do have $3 \times 6 = 18$ nodal degrees of freedom for $\mathbf{v}_h$ internal to three edges of triangle AEG, similar to (3.26) (see Figure 9), while q on the two sides of AEG has 18 nodal values (recall that for P_4, we have dimensions 9 and 10 for them.) But $\{\operatorname{div} \mathbf{v}_h\}$ is still short of one dimension.

Now, for all $k > 4$, we have $(k-4)$ mid-edge degrees of freedom on each edge, shown in Figure 9. We first construct a $\mathbf{v}_{3,m}$ to match q values at the $(k-4)$ mid-edge points. For example, for $k = 5$, on edge EA of Figure 8, we define

$$
\phi_{3,m} = \begin{cases} 16y(z-x)^2(1-z)^2 & \text{on } EAGH, \\ 16x(z-y)^2(1-z)^2 & \text{on } EAGF. \end{cases} \tag{3.31}
$$

Then the divergence of

$$
\mathbf{v}_{3,m} = q|_{EAGH}(0,0,\frac{1}{2}) \begin{pmatrix} 0 \\ \phi_{3,m} \\ 0 \end{pmatrix}
$$

is zero on all edges except on the side $EAGH$ of edge EA. As

$$
(q - \operatorname{div} \mathbf{v}_{3,m})_{EAGH}(0,0,\frac{1}{2}) = 0,
$$

we construct a $\mathbf{v}_h$ as (3.27)–(3.30) so that $\operatorname{div} \mathbf{v}_h|_{EAGH}$ matches $(q - \operatorname{div} \mathbf{v}_{3,m})_{EAGH}$ at two outside Lagrange nodes, $(0,0,\frac{1}{4})$ and $(0,0,\frac{3}{4})$. For $k > 5$, we have exact internal degrees of freedom for defining (3.31) to match q at internal edge nodes. Hence, a construction can be done for edges EA and AG for all $k \geq 4$.

Next, as in the last lemma, we have to preserve the mean divergence-zero elementwise by correcting $\operatorname{div} \mathbf{v}_3$ on three tetrahedra with two P_6 bubble functions, supported on two neighboring tetrahedra each, as (3.9). For example,

$$
\mathbf{b}_{3,0} = \begin{cases} c_0 \mathbf{n}_{AEG} L_{AEH}^2 L_{EGH}^2 L_{GAH}^2 & \text{on } EAGH, \\ \mathbf{n}_{AEG} L_{AEF}^2 L_{EGF}^2 L_{GAF}^2 & \text{on } EAGF. \end{cases}
$$

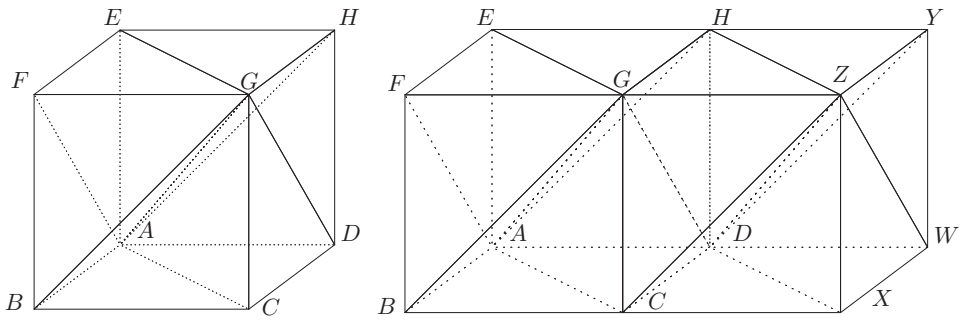

FIGURE 10. The interior and boundary vertices of Ω_h.

Here we need the divergence of P_6 bubble functions be zero at all vertices as well as on all edges.

Repeating this construction for each of the 6 triangles around the diagonal edge AG, we match q at all edges, assuming Ω_h has only 6 tetrahedra. For a general (small) cube $ABCDEFGH$ in a refined Ω_h, the cube has 6 two-tetrahedra edges like EA where two tetrahedra form a 90-degree face angle; cf. Figure 4. The above construction would match q exactly at 6 such two-tetrahedra edges. But the (small) cube $ABCDEFGH$ has also 6 one-tetrahedron edges like EH and 6 flat two-tetrahedra edges like EG (where two tetrahedra form a 180-degree face angle.) For these 6 one-tetrahedron and 6 flat two-tetrahedra edges, the above construction may not match $\operatorname{div} \mathbf{v}_{3,i}$ with q there. We need to construct further $\mathbf{v}_{3,i}$ for these two cases.

If EH is a boundary edge, but inside a face square, such as QP in Figure 4, then we use basis functions like (3.25), internal to triangle QPN to match $q|_{QP}$ at the bottom, to get a $\mathbf{v}_{3,b}$. Then $(q - \operatorname{div} \mathbf{v}_{3,b})$ would change the q values at the edge QP on the two tetrahedra inside the top cube, $QPNJ$ and $QPJH$. So we need to repeat the work in (3.25)–(3.30) on the triangle QPJ. Next, if EH is an internal edge, such as MN in Figure 4, the q values at edge MN are matched separately on the two cubes in front, and two cubes behind.

Finally, we consider the case of square-diagonal edge when it is not on the boundary, for example, EG in Figure 4. There, AH and GD are such singular edges in the other two directions. For simplicity of notation, we consider the case of GD depicted in Figure 10, where we assume D is the origin, and the two cubes sharing D are unit ones. Here GD is the intersection of two planes, $ZGAD$ and $HGCD$. We first see why it is called a singular edge. At any point $\mathbf{x}_0$ internal to the edge GD, for any $\mathbf{v}_h \in \mathbf{V}_{h,k}$, we write

$$\mathbf{v}_h = u_1 \begin{pmatrix} 0 \\ 1/\sqrt{2} \\ 1/\sqrt{2} \end{pmatrix} + u_2 \begin{pmatrix} 1 \\ 0 \\ 0 \end{pmatrix} + u_3 \begin{pmatrix} 0 \\ -1/\sqrt{2} \\ 1/\sqrt{2} \end{pmatrix} =: \mathbf{u}_1 + \mathbf{u}_2 + \mathbf{u}_3, \tag{3.32}$$

where u_1 is a global P_k polynomial on four tetrahedra sharing edge GD, while u_2 and u_3 are continuous piecewise-P_k on the four tetrahedra. By the continuity of

$\mathbf{v}_h$, we have

$$\begin{aligned}
&\operatorname{div}\mathbf{u}_1|_{AGDH}(\mathbf{x}_0) = \operatorname{div}\mathbf{u}_1|_{AGDC}(\mathbf{x}_0) = \operatorname{div}\mathbf{u}_1|_{ZGDH}(\mathbf{x}_0) = \operatorname{div}\mathbf{u}_1|_{ZGDC}(\mathbf{x}_0),\\
&\operatorname{div}\mathbf{u}_2|_{AGDH}(\mathbf{x}_0) = \operatorname{div}\mathbf{u}_2|_{ZGDH}(\mathbf{x}_0), \qquad \operatorname{div}\mathbf{u}_2|_{AGDC}(\mathbf{x}_0) = \operatorname{div}\mathbf{u}_2|_{ZGDC}(\mathbf{x}_0),\\
&\operatorname{div}\mathbf{u}_3|_{AGDH}(\mathbf{x}_0) = \operatorname{div}\mathbf{u}_3|_{AGDC}(\mathbf{x}_0), \qquad \operatorname{div}\mathbf{u}_3|_{ZGDH}(\mathbf{x}_0) = \operatorname{div}\mathbf{u}_3|_{ZGDC}(\mathbf{x}_0).
\end{aligned}$$

Therefore, the dimension of the linear vector space of

$$\{\operatorname{div}\mathbf{v}_h|_{AGDH}(\mathbf{x}_0), \operatorname{div}\mathbf{v}_h|_{AGDC}(\mathbf{x}_0), \operatorname{div}\mathbf{v}_h|_{ZGDH}(\mathbf{x}_0), \operatorname{div}\mathbf{v}_h|_{ZGDC}(\mathbf{x}_0)\} \tag{3.33}$$

is 3, not 4. Thus, for any point on edge GD, we have a checkerboard mode, which is limited by the constraint (cf. [11])

$$\sum_i (-1)^i \operatorname{div}\mathbf{v}_h|_{T_i}(\mathbf{x}_0) = 0, \tag{3.34}$$

where T_i stands for one of four tetrahedra around the edge GD. We need to construct local basis functions for each of three linearly independent vectors in (3.33). (3.32) provides a construction method. Let us consider first the P_4 case. Let

$$\phi_{3,s1} = \begin{cases} \frac{27}{4}(x-y)(z-x)(1-z)(1-z), & \text{on } ZGDH,\\ \frac{27}{4}x(z-x)(1+y-z)(1-z), & \text{on } AGDH, \end{cases} \tag{3.35}$$

$$\phi_{3,s2} = \begin{cases} \frac{27}{2}(x-y)(z-x)(1-z)x, & \text{on } ZGDH,\\ \frac{27}{2}x(z-x)(1+y-z)x, & \text{on } AGDH. \end{cases} \tag{3.36}$$

We next define

$$\mathbf{v}_{3,s1} = q|_{ZGDH}(\frac{1}{3},0,\frac{1}{3})\frac{1}{3}\begin{pmatrix} 0\\ 0\\ 4\phi_{3,s1}-\phi_{3,s2}\end{pmatrix},$$

$$\mathbf{v}_{3,s2} = q|_{ZGDH}(\frac{2}{3},0,\frac{2}{3})\frac{2}{3}\begin{pmatrix} 0\\ 0\\ \phi_{3,s2}-\phi_{3,s1}\end{pmatrix}.$$

Then, $\operatorname{div}(\mathbf{v}_{3,s1}+\mathbf{v}_{3,s2})$ matches q at the two Lagrange points on the edge GD, in $ZGDH$. Note that $\operatorname{div}(\mathbf{v}_{3,s1}+\mathbf{v}_{3,s2}) = 0$ at the two Lagrange points, on the other side of plane $AGDZ$. Similarly, we can define $\mathbf{v}_{3,s3}$ and $\mathbf{v}_{3,s4}$ so that their divergence matches q at the two Lagrange points inside $ZGDH$, while not altering the match done on the other side of plane $AGDZ$. Hence

$$q_3 := q - \operatorname{div}(\mathbf{v}_{3,s1}+\mathbf{v}_{3,s2}+\mathbf{v}_{3,s3}+\mathbf{v}_{3,s4}) \tag{3.37}$$

vanishes on the edge GD on $y>0$ side. As we did for the non-singular edge case AG, the construction (3.35)–(3.37) can be extended to any P_k, $k \geq 4$. Again, we correct q_3 on each element to keep (3.21) by P_6 bubble functions. By (3.34) and (3.37), edge GD behaves as a boundary edge for q_3. Hence the edge values of q_3 can be matched now by the divergence of $\mathbf{v}_{3,i}$, defined in (3.27), (3.29) and (3.30). Summing over all such $\mathbf{v}_{3,i}$ over all edges of Ω_h, after adding bubbles to preserve (3.21), denoted by $\mathbf{v}_3$, it satisfies (3.20)–(3.22). □

After we match the element integrals, the vertex values and the edge values of $q \in P_h$, we will next match q on each face of element. This is the simplest task among the others. The reason for this is that we can show the next lemma on any

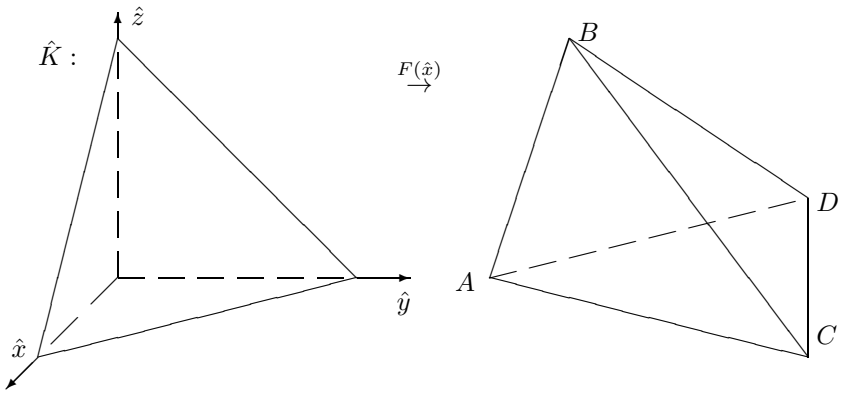

FIGURE 11. The affine mapping from $\hat{K}$ to K.

tetrahedral grid, unlike the other lemmas which are shown for the uniform grid only.

Lemma 3.4. *For any $q \in P_h$ defined in (2.4) such that $\int_K q = 0 \quad \forall K \in \Omega_h$, $k \geq 4$ and q vanishes at all edges of grid Ω_h, there is a function $\mathbf{v}_4 \in \mathbf{V}_{h,k}$ such that*

$$\operatorname{div} \mathbf{v}_4|_{T_i^K} = q|_{T_i^K} \quad \forall K \in \Omega_h, \tag{3.38}$$

$$\int_K \operatorname{div} \mathbf{v}_4 = 0 \quad \forall K \in \Omega_h, \tag{3.39}$$

$$\|\mathbf{v}_4\|_{H^1(\Omega)^3} \leq C\|q\|_{L^2(\Omega)}. \tag{3.40}$$

Here T_i^K, $1 \leq i \leq 4$, are the four face triangles of tetrahedron K.

Proof. We note that for $k = 1, 2, 3$, the lemma holds with $\mathbf{v}_4 = \mathbf{0}$ as $q \equiv 0$. To understand the analysis better, we first discuss the case $k = 4$, which is also covered in the proof for general $k \geq 4$ below. For $k = 4$, let $\mathbf{v}_4 = \mathbf{c}_0\phi_K$, where ϕ_K is the bubble function of P_4 on K. Then $\operatorname{div} \mathbf{v}_4$ is a P_3 function with zero integral on K and zero trace on the 6 edges of K. This is exactly how q is restricted in the lemma. The three choices in $\mathbf{c}_0$ for $\mathbf{v}_4$ will provide a unique match to the three degrees of freedom in defining q on K. We next formalize this argument rigorously for all $k \geq 4$.

For a given q specified in the lemma, we are going to construct $\mathbf{v}_4$ in 4 steps:

$$\mathbf{v}_4 = (\mathbf{v}_{4,1} + \mathbf{v}_{4,2} + \mathbf{v}_{4,3} + \mathbf{v}_{4,4})\phi_K \in C_0(K) \cap P_k^3, \tag{3.41}$$

where $\mathbf{v}_{4,i}$ are vector P_{k-4} polynomials to be specified and ϕ_K is the P_4 bubble function on K. Let $K = ABCD$ with 4 face triangles numbered as $T_1 = ABC$, $T_2 = ABD$, $T_3 = ACD$ and $T_4 = BCD$. Let $F(\hat{\mathbf{x}}) = B\hat{\mathbf{x}} + \mathbf{x}_0$ be an affine mapping from the reference tetrahedron $\hat{K} = \{0 \leq \hat{z} \leq 1-\hat{x}-\hat{y},\ 0 \leq y \leq 1-\hat{x},\ 0 \leq \hat{x} \leq 1\}$ to K so that the face triangles of $\hat{K}$ on the plane $\hat{x} = 0$, $\hat{y} = 0$, $\hat{z} = 0$ and $\hat{x}+\hat{y}+\hat{z} = 1$ are mapped to T_1, T_2, T_3 and T_4, respectively. This is shown in Figure 11. Mapping the equation $\operatorname{div}(\mathbf{v}_{4,4}) = q$ back to the reference element, we have

$$\hat{\mathbf{v}}_{4,4}^T B^{-T} \nabla \phi_{\hat{K}} + \phi_{\hat{K}} \operatorname{trace}\left(B^{-T} \nabla \hat{\mathbf{v}}_{4,4}\right) = \hat{q}(\hat{\mathbf{x}}), \tag{3.42}$$

where

$$\nabla\phi_{\hat{K}} = \begin{pmatrix} \hat{y}\hat{z}(1-2\hat{x}-\hat{y}-\hat{z}) \\ \hat{x}\hat{z}(1-\hat{x}-2\hat{y}-\hat{z}) \\ \hat{x}\hat{y}(1-\hat{x}-\hat{y}-2\hat{z}) \end{pmatrix}.$$

We choose, if $k > 4$,

$$\hat{\mathbf{v}}_{4,4} = B \begin{pmatrix} \hat{x} \\ \hat{y} \\ \hat{z} \end{pmatrix} u_4, \quad \text{for some } u_4 \in P_{k-5}. \tag{3.43}$$

Let $\hat{\mathbf{x}}_i = \langle \hat{x}_i, \hat{y}_i, \hat{z}_i \rangle$ be interior Lagrange points for P_{k-1} on the face triangle $\hat{T}_4 = F^{-1}(T_4)$ on the plane $\hat{x}+\hat{y}+\hat{z} = 1$ of the reference element. We derive the following from (3.42):

$$u_4(\hat{\mathbf{x}}_i) = -\frac{\hat{q}(\hat{\mathbf{x}}_i)}{\hat{x}_i\hat{y}_i\hat{z}_i}. \tag{3.44}$$

Since $\hat{q} = 0$ on the three edges of the triangle and mapping back to K, we conclude that

$$\begin{aligned} \operatorname{div} \mathbf{v}_{4,4}|_{T_4} &= q|_{T_4}, \\ \operatorname{div} \mathbf{v}_{4,4}|_{T_i} &= 0, \quad i \neq 1, \\ |\mathbf{v}_{4,4}|_{H^1} &\leq C\|q\|_{L^2}. \end{aligned}$$

Now, for $k = 4$ in (3.43), we have to match q on all four faces with only one $\mathbf{v}_{4,4}$ by letting

$$\hat{\mathbf{v}}_{4,4} = B\mathbf{c}_0, \quad \text{where } \mathbf{c}_0 = \left[\nabla\phi_{\hat{K}}(\hat{\mathbf{x}}_i)\right]^{-T} \begin{pmatrix} q(\hat{\mathbf{x}}_1) \\ q(\hat{\mathbf{x}}_2) \\ q(\hat{\mathbf{x}}_3) \end{pmatrix},$$

where $\hat{x}_i$ are the barycentric centers of any three-face triangle.

We repeat the construction of $\mathbf{v}_{4,4}$ three more times to get $\mathbf{v}_{4,1}$, $\mathbf{v}_{4,2}$, $\mathbf{v}_{4,3}$ in (3.41), whose divergence match q on the other three triangles. Similar to (3.43) we let

$$\hat{\mathbf{v}}_{4,1} = B \begin{pmatrix} 1-\hat{x}-\hat{y}-\hat{z} \\ 0 \\ 0 \end{pmatrix} u_1, \quad \text{for some } u_1 \in P_{k-5},$$

$$\hat{\mathbf{v}}_{4,2} = B \begin{pmatrix} 0 \\ 1-\hat{x}-\hat{y}-\hat{z} \\ 0 \end{pmatrix} u_2, \quad \text{for some } u_2 \in P_{k-5},$$

$$\hat{\mathbf{v}}_{4,3} = B \begin{pmatrix} 0 \\ 0 \\ 1-\hat{x}-\hat{y}-\hat{z} \end{pmatrix} u_3, \quad \text{for some } u_3 \in P_{k-5},$$

where (cf. (3.44)) u_i are determined by the nodal values:

$$u_1(\hat{\mathbf{x}}_i) = \frac{\hat{q}(\hat{\mathbf{x}}_i)}{\hat{y}_i\hat{z}_i(1-\hat{y}_i-\hat{z}_i)^2} \quad \forall \hat{\mathbf{x}}_i \in \hat{T}_1^0,$$
$$u_2(\hat{\mathbf{x}}_i) = \frac{\hat{q}(\hat{\mathbf{x}}_i)}{\hat{x}_i\hat{z}_i(1-\hat{x}_i-\hat{z}_i)^2} \quad \forall \hat{\mathbf{x}}_i \in \hat{T}_2^0,$$
$$u_3(\hat{\mathbf{x}}_i) = \frac{\hat{q}(\hat{\mathbf{x}}_i)}{\hat{x}_i\hat{y}_i(1-\hat{x}_i-\hat{y}_i)^2} \quad \forall \hat{\mathbf{x}}_i \in \hat{T}_3^0.$$

By the inverse reference mapping, we get $\mathbf{v}_{4,i}$. Letting $\mathbf{v}_4 = \sum_{i=1}^4 \mathbf{v}_{4,i}$. The lemma is proven. □

Lemma 3.5. *Let $q \in P_h$ defined in (2.4) with $k \geq 4$ such that $\int_K q = 0 \quad \forall K \in \Omega_h$ and q vanishes on all triangular faces of grid Ω_h. There is a function $\mathbf{v}_5 \in \mathbf{V}_{h,k}$ such that*

$$\operatorname{div} \mathbf{v}_5(x,y) = q(x,y) \quad \forall (x,y) \in \Omega, \tag{3.45}$$
$$\mathbf{v}_5(x,y) = 0 \quad \forall (x,y) \in \partial K \text{ and } \forall K \in \Omega_h, \tag{3.46}$$
$$\|\mathbf{v}_5\|_{H^1(\Omega)^3} \leq C\|q\|_{L^2(\Omega)}. \tag{3.47}$$

Proof. Each $K \in \Omega_h$ is a scaling of one of 6 unit tetrahedra shown in Figure 4. The properties listed in (3.45)–(3.47) are independent of scaling. Because we can work out the other 5 cases similarly, we show one case in which K is the unit tetrahedron $AEGH$ shown in Figure 4:

$$K = AEGH = \{(x,y,z) \mid 0 \leq x \leq y,\ 0 \leq y \leq z,\ 0 \leq z \leq 1\}.$$

When restricted on K, we let the pressure space satisfying the lemma be

$$P_K = \left\{ q \in P_{k-1}(K) \;\middle|\; \int_K q = 0,\ q|_{\partial K} = 0 \right\}. \tag{3.48}$$

For any $q_0 \in P_K$, we have

$$q_0 = \phi_K q_1, \quad \text{for some } q_1 \in P_{k-5}, \tag{3.49}$$

where ϕ_K is the degree-4 polynomial bubble function:

$$\phi_K = \lambda_1\lambda_2\lambda_3\lambda_4, \quad \text{where} \tag{3.50}$$
$$\lambda_1 = x, \quad \lambda_2 = y - x, \quad \lambda_3 = z - y, \quad \text{and} \quad \lambda_4 = 1 - \lambda_1 - \lambda_2 - \lambda_3 = 1 - z. \tag{3.51}$$

Further, $q = 0$ for any $k \leq 5$, due to $\int_K q = 0$, i.e., the lemma holds trivially for $4 \leq k \leq 5$. We next introduce a subspace of $H_0^1(K)^3 \cap P_k^3$ whose image under the divergence operator is inside the space P_K defined in (3.48):

$$\mathbf{V}_K = \left\{ \mathbf{v} \in P_k(K)^3 \;\middle|\; \mathbf{v}|_{\partial K} = 0,\ \operatorname{div} \mathbf{v} \in P_K \right\}. \tag{3.52}$$

We show next that the divergence operator is also an onto mapping from $\mathbf{V}_K$ to P_K. Because of divergence-free polynomials, we would reduce the space $\mathbf{V}_K$ to a much smaller one which is mapped to the space P_K one-to-one by the divergence operator. To make $\operatorname{div} \mathbf{v} \in P_K$, we can limit

$$\mathbf{v} = \phi_K \begin{pmatrix} \lambda_1\lambda_2 v_1(\lambda_1,\lambda_2,\lambda_3) \\ \lambda_2\lambda_3 v_2(\lambda_1,\lambda_2,\lambda_3) \\ \lambda_3\lambda_4 v_3(\lambda_1,\lambda_2,\lambda_3) \end{pmatrix} \quad \text{where } v_i \in P_{k-6}(\lambda_1,\lambda_2,\lambda_3),$$

so that $\operatorname{div}\mathbf{v}|_{\partial K} = \mathbf{0}$. This can be seen by the calculation (3.54) below. After eliminating divergence-free functions, we let

$$\mathbf{V}_0 = \left\{ \mathbf{v} \in P_k(K)^3 \;\middle|\; \mathbf{v} = \phi_K \begin{pmatrix} \lambda_1\lambda_2 v_1(\lambda_1,\lambda_2,\lambda_3) \\ \lambda_2\lambda_3 v_2(\lambda_1,\lambda_3) \\ \lambda_3\lambda_4 v_3(\lambda_1) \end{pmatrix},\ v_i \in P_{k-6}(K)^{4-i} \right\}. \tag{3.53}$$

Indeed, we have $\operatorname{div}\mathbf{v}_0 \in P_K$ for $\mathbf{v}_0 \in \mathbf{V}_0$, as

$$\begin{aligned} \operatorname{div}\mathbf{v}_0 = \phi_K[&2(\lambda_2-\lambda_1)v_1 + \lambda_1\lambda_2 v_{1x} + 2(1-\lambda_1-2\lambda_2-\lambda_3)v_2 \\ &+ 2v_3(\lambda_1+\lambda_2+2\lambda_3-1)]. \end{aligned} \tag{3.54}$$

Now, for each $q_0 \in P_K$, we will find a $\mathbf{v}_0 \in \mathbf{V}_0$ such that $\operatorname{div}\mathbf{v}_0 = q_0$. This is done by mathematical induction. We first construct a $\mathbf{v}_0$ such that the highest order terms of $\operatorname{div}\mathbf{v}_0$ match those of a given $q_0 \in P_K$. For any $q_0 \in P_K$, we separate the degree $k-5$ terms of q_1 in (3.48) from the rest as follows:

$$q_1 = \sum_{i=0}^{k-5}\sum_{j=0}^{k-5-i}\sum_{l=k-5-i-j} q_{ijl}\lambda_1^i\lambda_2^j\lambda_3^l + q_2(\lambda_1,\lambda_2,\lambda_3), \tag{3.55}$$

where q_2 is a degree $(k-6)$ polynomial. When we compare the degree $k-5$ terms of $\operatorname{div}\mathbf{v}_0$ in (3.54) and q_1 in (3.55), we need to check only the degree $(k-6)$ terms in v_1, v_2 and v_3. We let a $\mathbf{v}_0$ in (3.53) be

$$\begin{aligned} v_1(\lambda_1,\lambda_2,\lambda_3) &= \sum_{i=0}^{k-6}\sum_{j=0}^{k-6-i}\sum_{l=k-6-i-j} && v_{1,ijl} \quad \lambda_1^i\lambda_2^j\lambda_3^l, \\ v_2(\lambda_1,\lambda_3) &= \sum_{i=0}^{k-6}\sum_{l=k-6-i} && v_{2,i0l} \quad \lambda_1^i\lambda_3^l, \\ v_3(\lambda_1) &= \sum_{i=k-6} && v_{3,i00} \quad \lambda_1^i. \end{aligned} \tag{3.56}$$

We note that there are

$$\sum_{i=0}^{k-5}\sum_{j=0}^{k-5-i} 1 = \sum_{i=0}^{k-5}(i+1) = \frac{(k-3)(k-4)}{2}$$

coefficients of q_{ijl} in (3.55), which defines the $(k-3)(k-4)/2$ linear equations for the unknown coefficients of v_i in (3.56):

$$(\sum_{i=0}^{k-6}\sum_{j=0}^{k-6-i} 1) + (\sum_{i=0}^{k-6} 1) + 1 = \frac{(k-4)(k-5)}{2} + k - 5 + 1 = \frac{(k-3)(k-4)}{2}.$$

We can list the $(k-3)(k-4)/2$ linear equations in the following order to get an upper triangular system except the last three equations involving $v_{1,(k-6)00}$, $v_{2,(k-6)00}$ and $v_{3,(k-6)00}$:

For $i = 0$,

$$-2v_{2,00(l-1)} = q_{ijl}, \qquad j = 0, \tag{3.57}$$

$$2v_{1,00l} = q_{ijl} + 4v_{2,00l}, \qquad j = 1, \tag{3.58}$$

$$2v_{1,0(j-1)l} = q_{ijl}, \qquad j = 2 : (k-5). \tag{3.59}$$

For $i = 1 : (k-7)$,

$$-2v_{2,i0(l-1)} = q_{ijl} + 2v_{1,(i-1)0l} - 2v_{2,(i-1)0l}, \qquad j = 0, \tag{3.60}$$

$$(2+i)v_{1,i0l} = q_{ijl} + 2v_{1,(i-1)1l} + 4v_{2,i0l}, \qquad j = 1, \tag{3.61}$$

$$(2+i)v_{1,i(j-1)l} = q_{ijl} + 2v_{1,(i-1)jl}, \qquad j = 2 : (k-5-i). \tag{3.62}$$

For $i = k-6$,

$$-2v_{2,i00} + 4v_{3,i00} = q_{ijl} + 2v_{1,(i-1)0l} - 2v_{2,(i-1)0l}, \qquad j = 0, \tag{3.63}$$

$$(2+i)v_{1,i00} + 2v_{3,i00} = q_{ijl} + 2v_{1,(i-1)1l} + 4v_{2,i0l}, \qquad j = 1. \tag{3.64}$$

Finally, for $i = k-5$,

$$-2v_{1,(i+1)00} - 2v_{2,(i+1)00} + v_{2,(i+1)00} = q_{ijl} + 2v_{1,(i-1)jl}. \tag{3.65}$$

Here in equations (3.57)–(3.65), the index $l = k-5-i-j$. Also in all of these equations, all $v_{m,ijl}$ on the right-hand side are resolved by earlier equations. For the last three equations (3.63)–(3.65), the determinant of the 3×3 coefficient matrix is $-4(k-6)$. So, for a $k \geq 7$, we find a unique $\mathbf{v}_0$ so that $\operatorname{div} \mathbf{v}_0$ and q_0 match the highest order terms. We move the $\operatorname{div} \mathbf{v}_0$ to the right-hand side of (3.48), combined into q_2 there. We then repeat the above construction for one lower degree q_0, until $k = 6$. When $k = 6$, the systems of equations (3.57)–(3.65) become to

$$\begin{aligned} -2v_{2,000} &= q_{001}, \\ 2v_{1,000} &= q_{010} + 4v_{2,000}, \\ 2v_{3,000} &= q_{100} + 2v_{1,000} + 2v_{2,000}. \end{aligned}$$

This system is an upper triangular one, and has a unique solution.

Therefore, we constructed a locally supported $\mathbf{v}_5$ on one tetrahedron $AEGH$. Similar construction can be done on the other five types of tetrahedra. The lemma is proven. □

Corollary 3.1. *Let $k \geq 6$. The mixed finite element pair $(\mathbf{V}_{h,k}, P_h)$ are defined in* (2.3) *and* (2.4). *Let n be the number of cubes in each coordinate direction; cf. Figure* 2. *The dimensions of $\mathbf{V}_{h,k}$, P_h and subspace $\mathbf{Z}_h$ (defined in* (2.8)) *are*

$$\dim V_{h,k} = (nk-1)^3, \tag{3.66}$$

$$\dim P_h = \frac{1}{6}n^3(k+2)(k+1)k - 3kn(n^2+n+2) + 5, \tag{3.67}$$

$$\dim \mathbf{Z}_h = \dim V_{h,k} - \dim P_h. \tag{3.68}$$

Proof. We summarize all constraints for $\operatorname{div} \mathbf{w}_h = q$ in the last few lemmas:

Corner vertices – Type (b):	2×6,
Corner vertices – Type (a):	3×2,
Mid-edge vertices – Type (c):	$4 \times 6(n-1)$,
Mid-edge vertices – Type (d):	$3 \times 6(n-1)$,
Mid-face vertices – Type (e):	$4 \times 6(n-1)^2$,
Internal vertices – Type (f):	$6 \times (n-1)^3$,
One-tetrahedron boundary edges:	$(k-2) \times 6n$,
Diagonal boundary edges:	$(k-2) \times 6n^2$,
Internal singular edges:	$(k-2) \times 3(n-1)n^2$,
Global integral constraint:	1.

Deducting the number of constraints from the dimension of discontinuous P_{k-1} polynomials on Ω_h, we prove the corollary. □

Numerically, we have verified Corollary 3.1:

$$\dim P_h = \begin{cases} 269 & \text{if } k = 6,\ n = 1, \\ 2405 & \text{if } k = 6,\ n = 2, \\ 425 & \text{if } k = 7,\ n = 1, \\ 3701 & \text{if } k = 7,\ n = 2. \end{cases}$$

We proved (3.67) for $k \geq 6$ only, but it seems to hold for $k = 5$ as well:

$$\dim P_h = 155 \text{ and } 1445, \text{ if } n = 1 \text{ and } 2, \text{ respectively.}$$

However, (3.67) no longer holds for $k \leq 4$:

$$\dim P_h = 75 \text{ and } 772, \text{ if } n = 1 \text{ and } 2, \text{ respectively,}$$

while (3.67) gives 76 and 789, respectively.

Theorem 3.1. *Let $k \geq 6$. The mixed finite element pair $(\mathbf{V}_{h,k}, P_h)$ defined in* (2.3) *and* (2.4) *is stable on the uniform grids, i.e., the following inf-sup condition holds:*

$$\inf_{q \neq 0, q \in P_h} \sup_{\mathbf{v}_h \in \mathbf{V}_{h,k}} \frac{b(\mathbf{v}_h, q)}{\|\mathbf{v}_h\|_{H^1(\Omega)^3} \|q\|_{L^2(\Omega)}} \geq C. \tag{3.69}$$

Proof. For any $q \in P_h$, we construct a $\mathbf{v}_h \in \mathbf{V}_{h,k}$ to satisfy (3.69). By (3.1), there is a $\mathbf{v}_1 \in \mathbf{V}_h$ such that

$$\int_K (q - \operatorname{div} \mathbf{v}_1) = 0 \quad \forall K \in \Omega_h,$$
$$\|\mathbf{v}_1\|_{H^1} \leq C_1 \|q\|_{L^2}.$$

By (3.2), there is $\mathbf{v}_2 \in \mathbf{V}_h$ such that

$$[\operatorname{div} \mathbf{v}_2 - q + \operatorname{div} \mathbf{v}_1]|_K (a_i^K) = 0 \quad \forall K \in \Omega_h \text{ and for all vertices of } K,$$
$$\|\mathbf{v}_2\|_{H^1} \leq C_2 \|q - \operatorname{div} \mathbf{v}_1\|_{L^2}.$$

By (3.20), there is $\mathbf{v}_3 \in \mathbf{V}_h$ such that

$$[\operatorname{div} \mathbf{v}_3 - q + \operatorname{div}(\mathbf{v}_1 + \mathbf{v}_2)]|_K (E_i^K) = 0 \quad \forall K \in \Omega_h \text{ and for all edges of } K,$$
$$\|\mathbf{v}_3\|_{H^1} \le C_3 \|q - \operatorname{div}(\mathbf{v}_1 - \mathbf{v}_2)\|_{L^2}.$$

By (3.38), there is $\mathbf{v}_4 \in \mathbf{V}_h$ such that

$$[\operatorname{div} \mathbf{v}_4 - q + \operatorname{div}(\mathbf{v}_1 + \mathbf{v}_2 + \mathbf{v}_3)]|_K (F_i^K) = 0 \quad \forall K \in \Omega_h$$
$$\text{and for all face triangles of } K,$$
$$\|\mathbf{v}_4\|_{H^1} \le C_4 \|q - \operatorname{div}(\mathbf{v}_1 + \mathbf{v}_2 + \mathbf{v}_3)\|_{L^2}.$$

By (3.45), there is a $\mathbf{v}_5 \in \mathbf{V}_h$ such that

$$\operatorname{div} \mathbf{v}_5 = q - \operatorname{div}(\mathbf{v}_1 + \mathbf{v}_2 + \mathbf{v}_3 + \mathbf{v}_4),$$
$$\|\mathbf{v}_5\|_{H^1} \le C_5 \|q - \operatorname{div}(\mathbf{v}_1 + \mathbf{v}_2 + \mathbf{v}_3 + \mathbf{v}_4)\|_{L^2}.$$

Let $\mathbf{v} = -\mathbf{v}_1 - \mathbf{v}_2 - \mathbf{v}_3 - \mathbf{v}_4 - \mathbf{v}_5$. It follows that

$$\begin{aligned}
\|\mathbf{v}\|_{H^1} &\le \|\mathbf{v}_1\|_{H^1} + \|\mathbf{v}_2\|_{H^1} + \|\mathbf{v}_3\|_{H^1} + \|\mathbf{v}_4\|_{H^1} + \|\mathbf{v}_5\|_{H^1} \\
&\le C_1 \|q\|_{L^2} + C_2 \|q - \operatorname{div} \mathbf{v}_1\|_{L^2} + C_3 \|q - \operatorname{div}(\mathbf{v}_1 + \mathbf{v}_2)\|_{L^2} + \cdots \\
&\le C_1 \|q\|_{L^2} + C_2 (\|q\|_{L^2} + \|\operatorname{div} \mathbf{v}_1\|_{L^2}) + \cdots \\
&\le C_1 \|q\|_{L^2} + C_2 (\|q\|_{L^2} + C_1 \|q\|_{L^2}) + \cdots \\
&\le C_* \|q\|_{L^2}
\end{aligned}$$

and that

$$b(\mathbf{v}_h, q) = (-\operatorname{div} \mathbf{v}_h, q) = \|q\|^2_{L^2(\Omega)} \ge C_*^{-1} \|\mathbf{v}\|_{H^1(\Omega)^3} \|q\|_{L^2(\Omega)}.$$

(3.69) is proved with $C = C_*^{-1}$. □

Theorem 3.2. *Let $k \ge 6$. The discrete solution $(\mathbf{u}_h, p_h)$ of (2.5) approximate that of (2.2) in the optimal order:*

$$\|\mathbf{u} - \mathbf{u}_h\|_{H^1(\Omega)^3} + \|p - p_h\|_{L^2(\Omega)} \le C h^{\min\{k,r\}} (\|\mathbf{u}\|_{H^{r+1}(\Omega)^3} + \|p\|_{H^r(\Omega)}), \quad r \ge 1. \tag{3.70}$$

Proof. By the inf-sup condition (3.69) and the standard mixed finite element theory [10], it follows that

$$\begin{aligned}
&\|\mathbf{u} - \mathbf{u}_h\|_{H^1(\Omega)^3} + \|p - p_h\|_{L^2(\Omega)} \\
&\quad \le C \Big(\inf_{\mathbf{v}_h \in \mathbf{V}_{h,k}} \|\mathbf{u} - \mathbf{v}_h\|_{H^1(\Omega)^3} + \inf_{q_h \in P_h} \|p - q_h\|_{L^2(\Omega)} \Big) \\
&\quad \le C \Big(\inf_{\mathbf{v}_h \in \mathbf{V}_{h,k}} \|\mathbf{u} - \mathbf{v}_h\|_{H^1(\Omega)^3} + \inf_{q_h \in \tilde{P}_h} \|p - q_h\|_{L^2(\Omega)} \Big)
\end{aligned}$$

where $\tilde{P}_h$ is the space of continuous P_{k-1} polynomials with mean value zero:

$$\tilde{P}_h = P_h \cap C(\Omega) = \left\{ q_h \in C(\Omega) \mid \int_\Omega q_h = 0,\ q_h|_K \in P_{k-1}\ \forall K \in \Omega_h \right\}.$$

The theorem is proven as both spaces $\mathbf{V}_{h,k}$ and $\tilde{P}_h$ provide the optimal order of approximation. □

4. Numerical tests

In this section, we report some numerical tests on the P_k-P_{k-1} elements for the stationary Stokes equations (2.1) on the unit cube, $\Omega = (0,1)^3$. The grids are obtained by the standard multigrid refinement; cf. [16]. The first three grids are depicted in Figure 2.

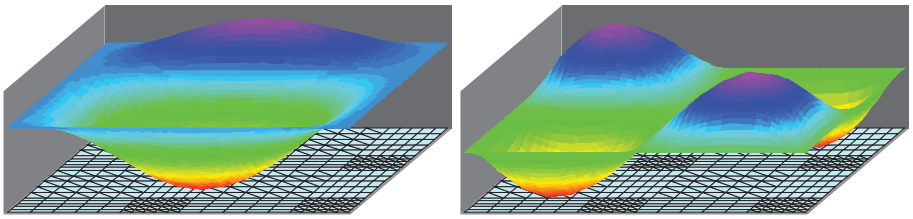

FIGURE 12. The exact solution, the first component of $\mathbf{u}$ and p in (4.2), restricted on $z = 0.33$.

We choose the right-hand side function $\mathbf{f}$ for (2.1) as

$$\begin{aligned}\mathbf{f} &= -\Delta\,\mathbf{curl}\begin{pmatrix}0\\ g\\ g\end{pmatrix} + \frac{1}{9}\nabla g_{xy}\\ &= \begin{pmatrix}-g_{xxy} - g_{yyy} - g_{yzz} + g_{xxz} + g_{yyz} + g_{zzz} + g_{xxy}/9\\ -g_{xxx} - g_{xyy} - g_{xzz} + g_{xyy}/9\\ g_{xxx} + g_{xyy} + g_{xzz} + g_{xyz}/9\end{pmatrix},\end{aligned} \tag{4.1}$$

where

$$g = 2^{12}(x - x^2)^2(y - y^2)^2(z - z^2)^2.$$

The exact solution for the Stokes equations (2.1) is

$$\mathbf{u} = \mathbf{curl}\begin{pmatrix}0\\ g\\ g\end{pmatrix}, \quad p = \frac{1}{9}g_{xy}. \tag{4.2}$$

As we are unable to plot a 3D function in 4D, we show the restriction of the functions $\mathbf{u}$ (the first component) and p, on the plane $z = 0.33$ in Figure 12. We note that the grids obtained by the intersection of tetrahedra in Ω_h and the plane consist of both rectangles and triangles, shown at the bottom in Figure 12 and in Figure 13.

In Table 1 we list errors for the P_k-P_{k-1} element for $k = 6$, on three level of grids Ω_h. The iterated penalty method is used to solve the discrete linear equations. The order of convergence fits the estimate (3.70) well. We show some errors in Figure 14.

TABLE 1. The errors for the P_k-P_{k-1} ($k = 6$) element on Figure 2 grids.

	$\lvert\mathbf{u} - \mathbf{u}_h\rvert_{H^1}$	h^n	$\lVert p - p_h\rVert_{L^2}$	h^n
1	6.73310		29.66007	
2	0.23981	4.81	1.13377	4.70
3	0.00421	5.83	0.02196	5.69

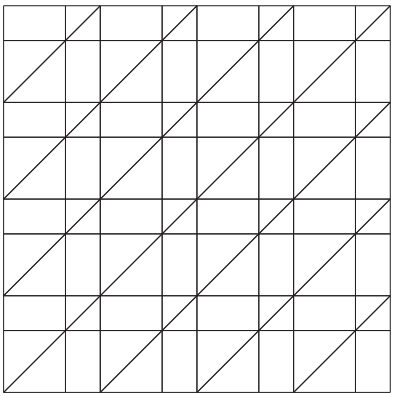

FIGURE 13. The cut on the third level grid Ω_h by plane $z = 0.33$.

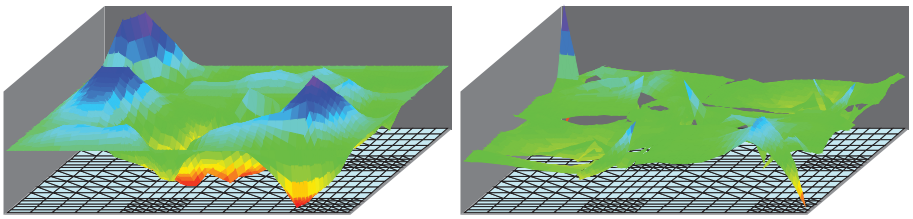

FIGURE 14. The errors for the first component of $\mathbf{u}$ and p restricted on plane $z = 0.33$.

ACKNOWLEDGMENTS

This work was initially supported by the National Science Foundation Award 9625907 and finished in June 2008 during the author's visit to Dr. Xuejun Xu, sponsored by the State Key Laboratory of Scientific and Engineering Computing, Beijing, China.

The author thanks an anonymous referee who pointed out numerous mistakes in an early version of this manuscript.

REFERENCES

[1] D. N. Arnold and J. Qin, *Quadratic velocity/linear pressure Stokes elements*, in Advances in Computer Methods for Partial Differential Equations VII, R. Vichnevetsky and R.S. Steplemen, eds., 1992.

[2] D. Boffi, *Three-dimensional finite element methods for the Stokes problem,* SIAM J. Numer. Anal. 34 (1997), 664–670. MR1442933 (98a:65160)

[3] S. C. Brenner and L. R. Scott, The Mathematical Theory of Finite Element Methods, Springer-Verlag, New York, 1994. MR1278258 (95f:65001)

[4] F. Brezzi and M. Fortin, Mixed and hybrid finite element methods, Springer, 1991. MR1115205 (92d:65187)

[5] P.G. Ciarlet, The Finite Element Method for Elliptic Problems, North-Holland, Amsterdam, 1978. MR0520174 (58:25001)

[6] M. Fortin and R. Glowinski, Augmented Lagrangian Methods: Applications to the Numerical Solution of Boundary-value Problems, North Holland, Amsterdam, 1983. MR724072 (85a:49004)

[7] J. Pitkäranta and R. Stenberg, *Error bounds for the approximation of the Stokes problem using bilinear/constant elements on irregular quadrilateral meshes*, in The Mathematics of finite elements and applications V, J. Whiteman, ed., Academic Press, London, 1985, 325–334. MR811045

[8] J. Qin, On the convergence of some low order mixed finite elements for incompressible fluids, Thesis, Pennsylvania State University, 1994.

[9] J. Qin and S. Zhang, *Stability and approximability of the P1-P0 element for Stokes equations*, Int. J. Numer. Meth. Fluids **54** (2007), no. 5, 497–515. MR2322456 (2008b:65153)

[10] P. A. Raviart and V. Girault, Finite element methods for Navier-Stokes equations, Springer, 1986. MR851383 (88b:65129)

[11] L. R. Scott and M. Vogelius, *Norm estimates for a maximal right inverse of the divergence operator in spaces of piecewise polynomials*, RAIRO, Modelisation Math. Anal. Numer. 19 (1985), 111–143. MR813691 (87i:65190)

[12] L. R. Scott and M. Vogelius, *Conforming finite element methods for incompressible and nearly incompressible continua*, in Lectures in Applied Mathematics 22, 1985, 221–244. MR818790 (87h:65202)

[13] L. R. Scott and S. Zhang, *Finite element interpolation of nonsmooth functions satisfying boundary conditions*, Math. Comp. 54 (1990), 483–493. MR1011446 (90j:65021)

[14] L. R. Scott and S. Zhang, Multilevel Iterated Penalty Method for Mixed Elements, the Proceedings for the Ninth International Conference on Domain Decomposition Methods, 133-139, Bergen, 1998.

[15] M. Vogelius, *A right-inverse for the divergence operator in spaces of piecewise polynomials application to the p version of the finite element method*, Numer. Math. 41 (1983), 19–37. MR696548 (85f:65113a)

[16] S. Zhang, *Successive subdivisions of tetrahedra and multigrid methods on tetrahedral meshes*, Houston J. of Math. 21 (1995), 541–556. MR1352605 (96f:65183)

[17] S. Zhang, *A new family of stable mixed finite elements for 3D Stokes equations*, Math. Comp. 74 (2005), 250, 543–554. MR2114637 (2005j:65151)

[18] S. Zhang, *On the P1 Powell-Sabin divergence-free finite element for the Stokes equations,* J. Comp. Math., 26 (2008), 456-470. MR2421893 (2009j:76160)

Department of Mathematical Sciences, University of Delaware, Newark, Delaware 19716

E-mail address: szhang@udel.edu